MRI and dynamo action

Action of differential rotation on large-scale magnetic field of stars and planets

Ludovic Petitdemange
Max-Planck Insitut für Astronomie
(MPIA-Heidelberg)

Martin Schrinner
Emmanuel Dormy
Steven Balbus
Hubert Klahr

Eilat WIZAP Workshop 2011

Contents

- Introduction
  - Magnetic fields in astrophysics
  - Evidence for differential rotation
  - Origin of magnetic fields : Dynamo action
  - Weak fields on differentially rotating systems (MRI)
- From the planets to the stars
  - Two distinct regimes: dipolar vs oscillatory dynamos
  - Numerical model of oscillaroty dynamo
  - Generalization and futur developments
- MRI in planetary interiors

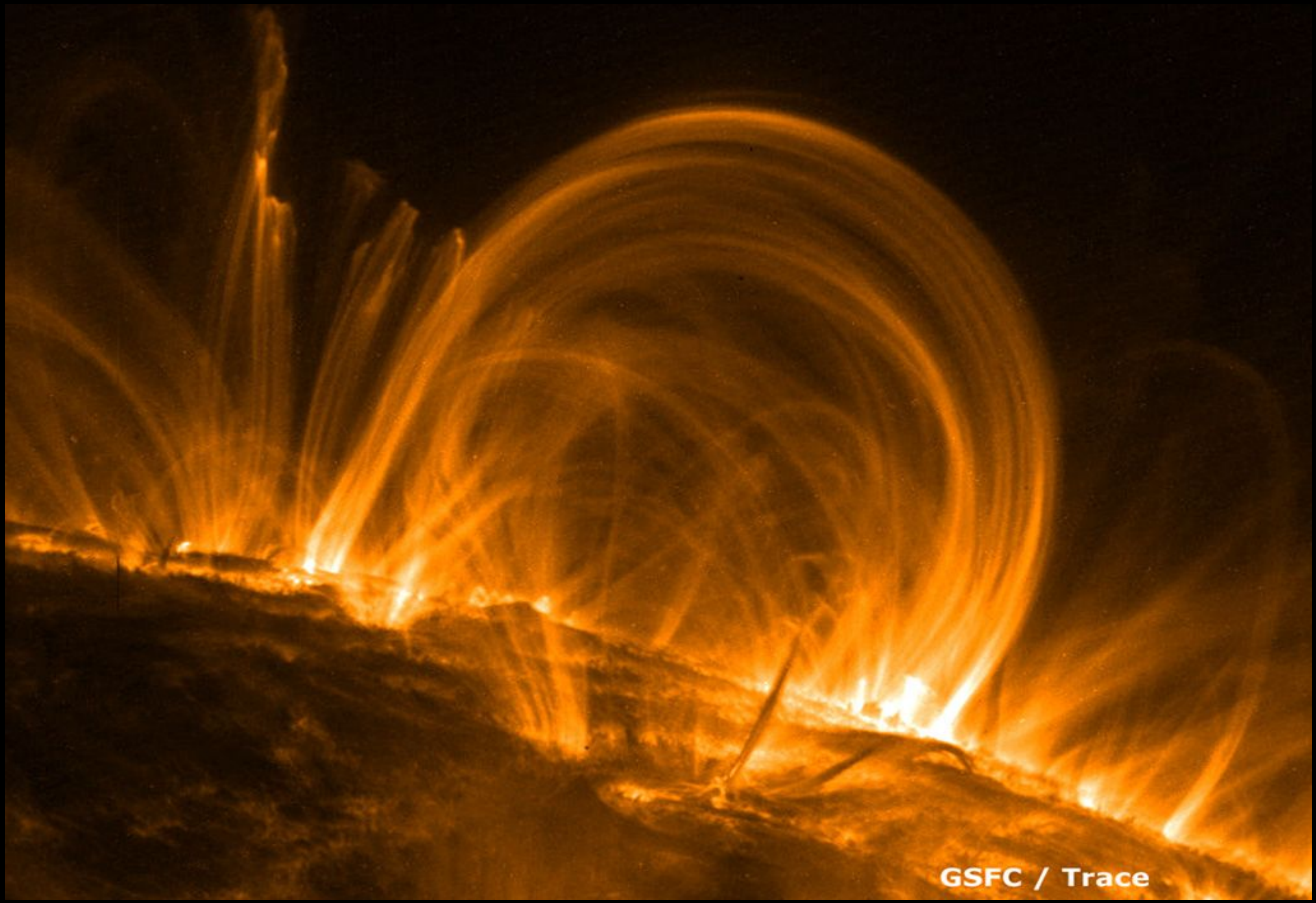

Planetary magnetic fields in our solar system

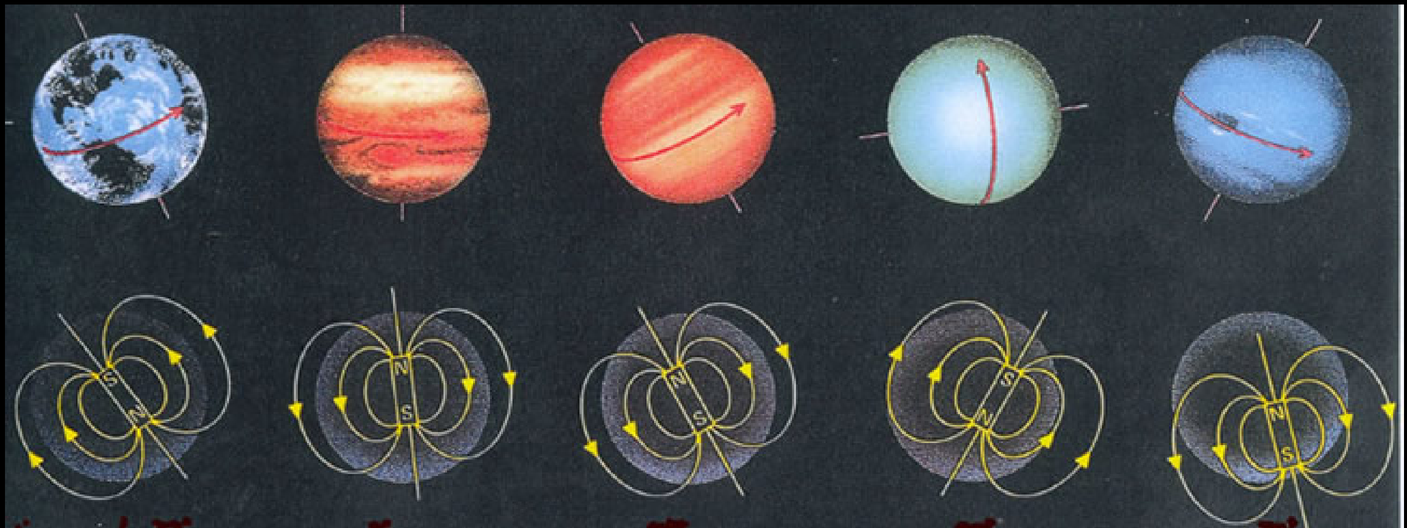

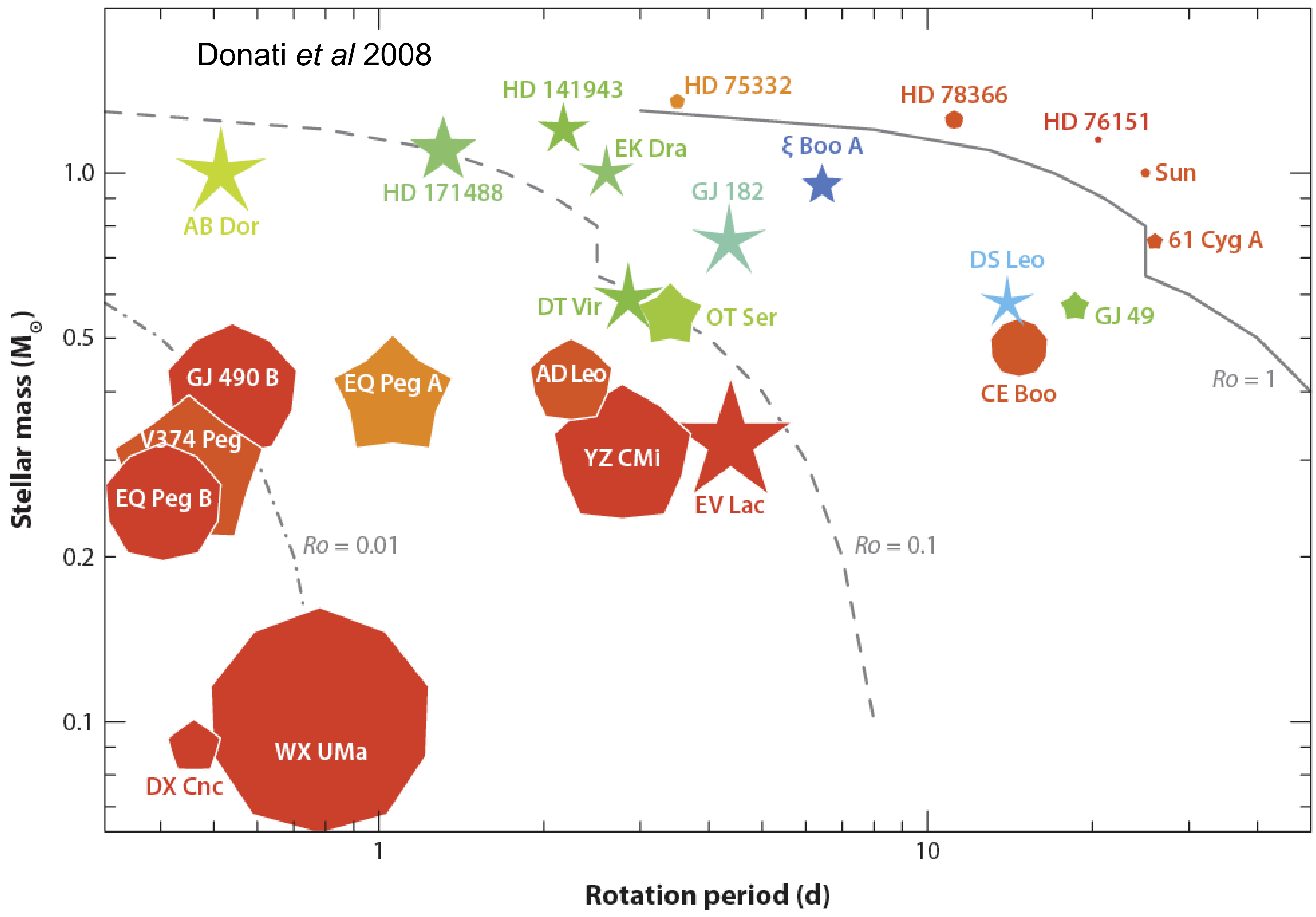
Donati et al 2008
HD 141943
HD 75332
HD 78366
HD 76151
AB Dor
HD 171488
EK Dra
ξ Boo A
Sun
GJ 182
61 Cyg A
DS Leo
DT Vir
OT Ser
GJ 49
GJ 490 B
EQ Peg A
AD Leo
CE Boo
Ro = 1
V374 Peg
YZ CMi
EQ Peg B
EV Lac
Ro = 0.01
Ro = 0.1
WX UMa
DX Cnc
1.0
0.5
0.2
0.1
1
10
Stellar mass (M⊙)
Rotation period (d)

Oscillatory Dynamos

Solar dynamo: 11-year activity cycle

Butterfly diagram

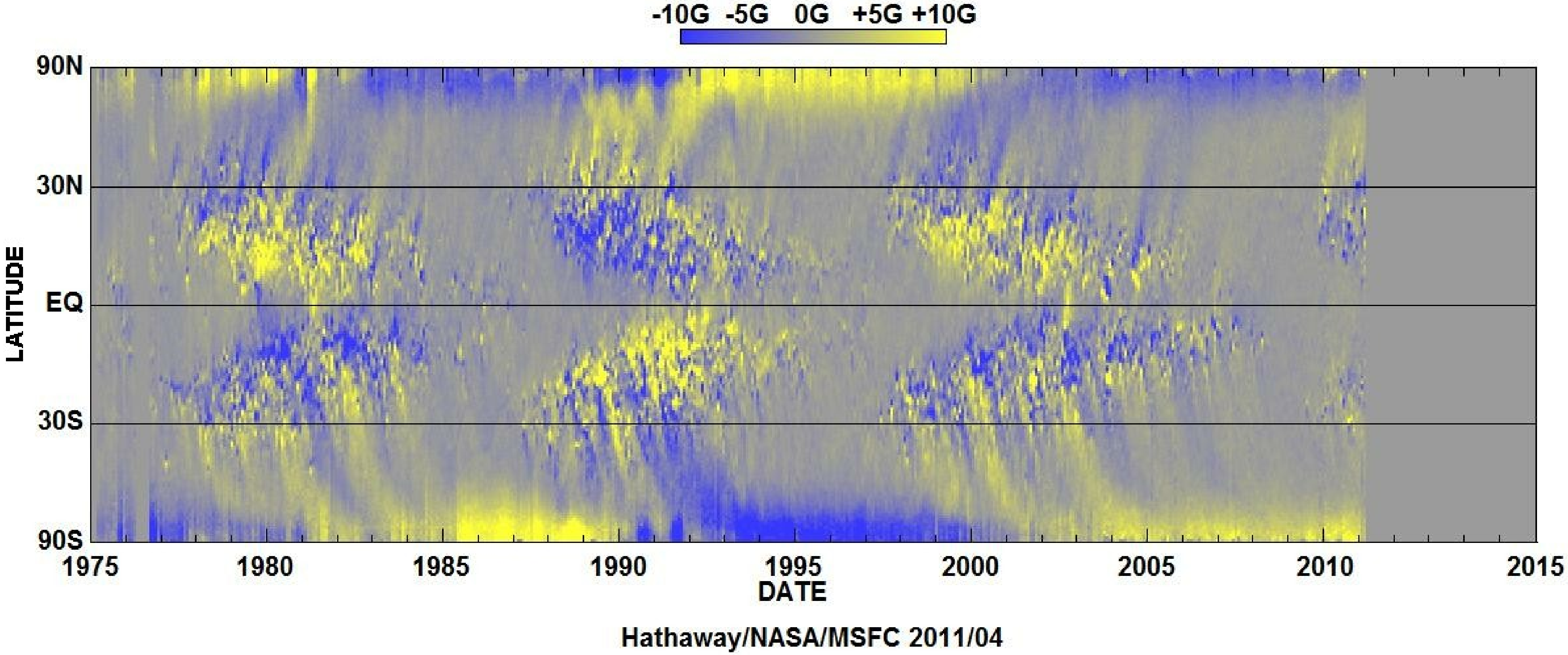

Earth's field variations

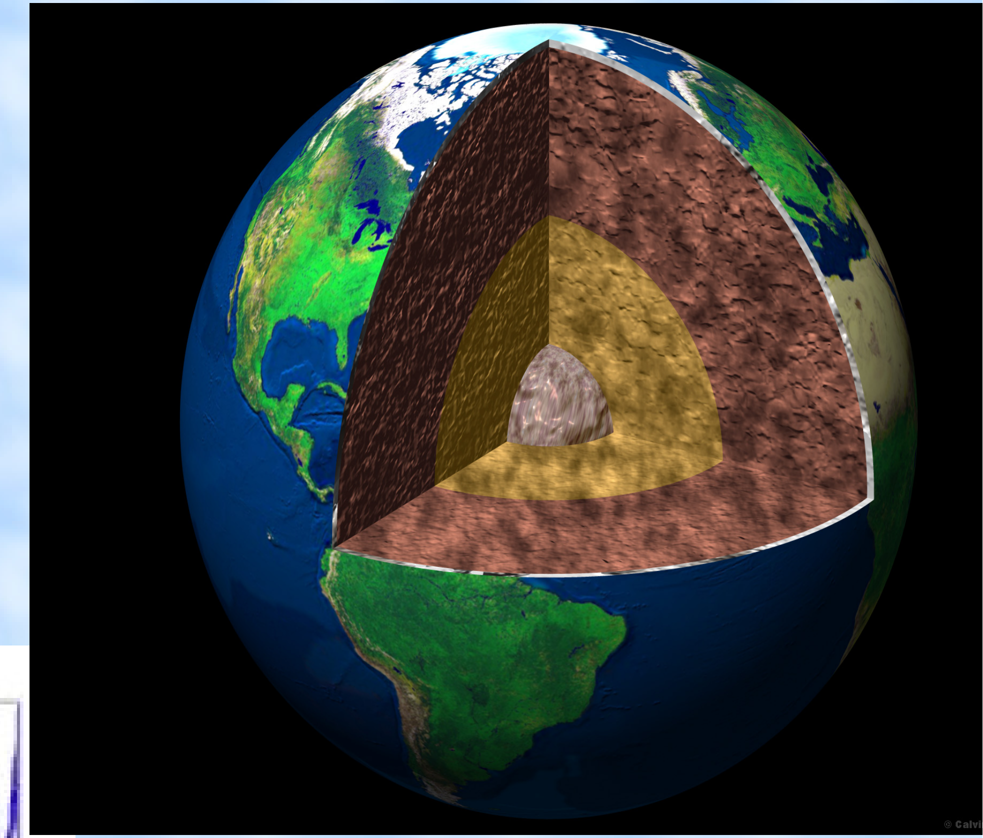

Measured Intensity

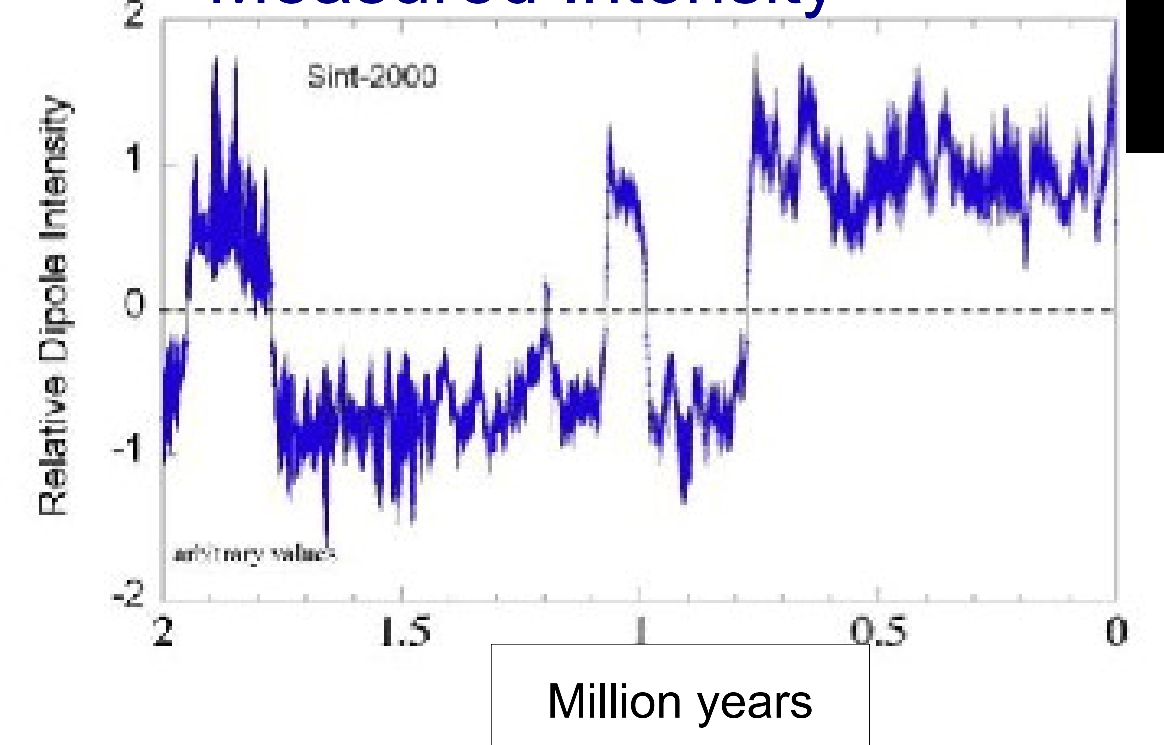

Variations on
Different timescales

Jerks (Magnetic impulses) on
only a few months
(Olsen et al 2008).

Observations of Differential Rotation

- Planetary interiors
  - Earth's outer core

    Seismologycal data: inner core rotation 0.15^{o} per year.
  - Jupiter and Saturn

- Stellar interiors

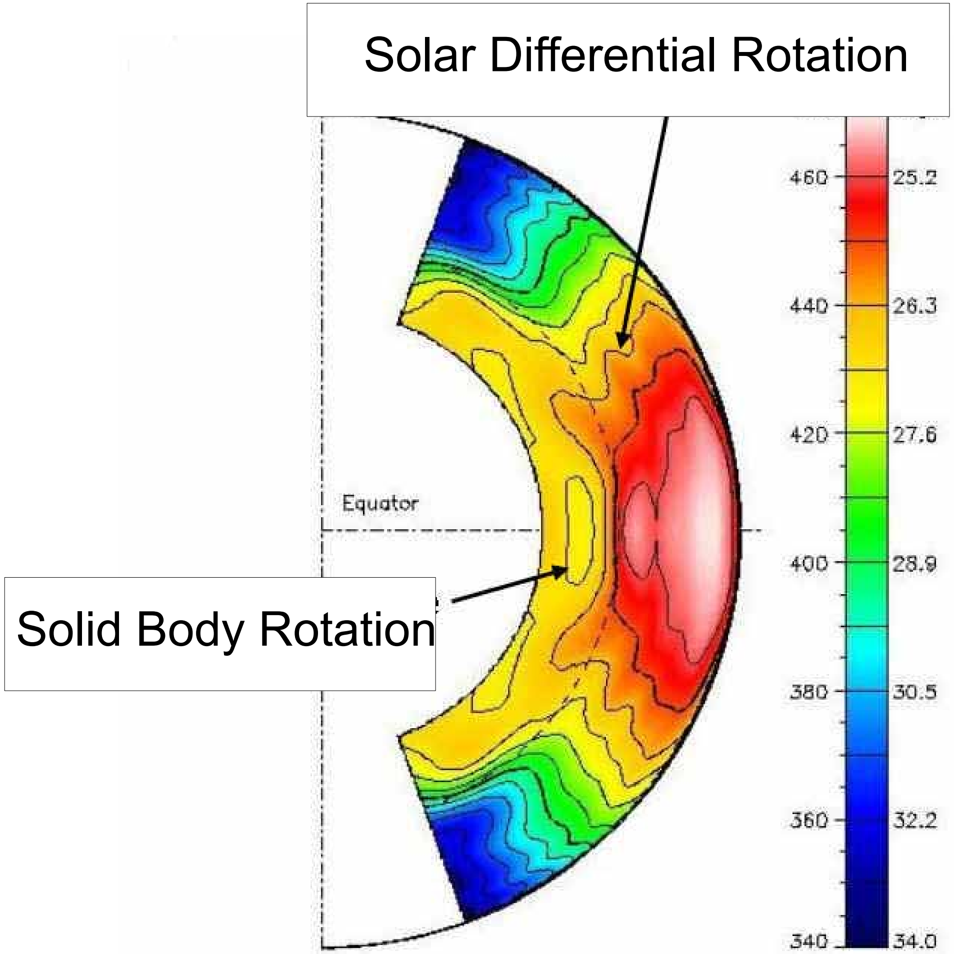

Kinematic dynamo

Poloidal magnetic field lines are distorted by differential rotation into toroidal magnetic field.

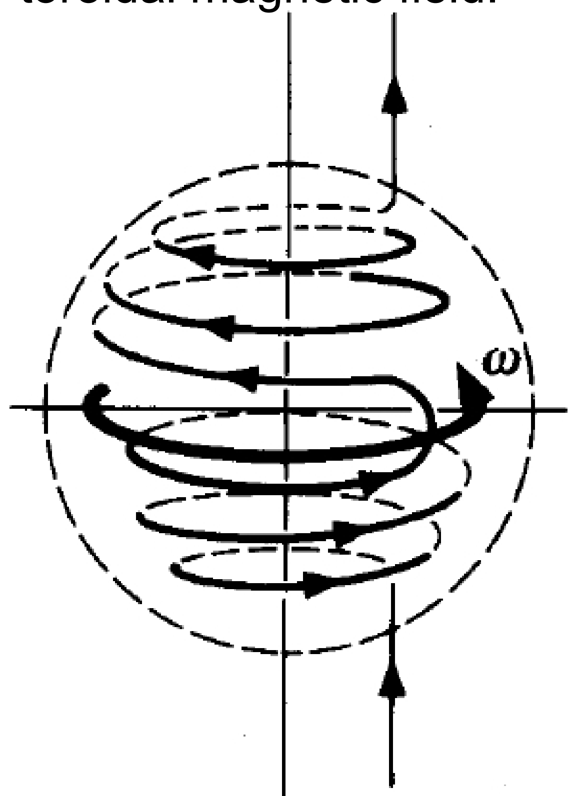

ω effect

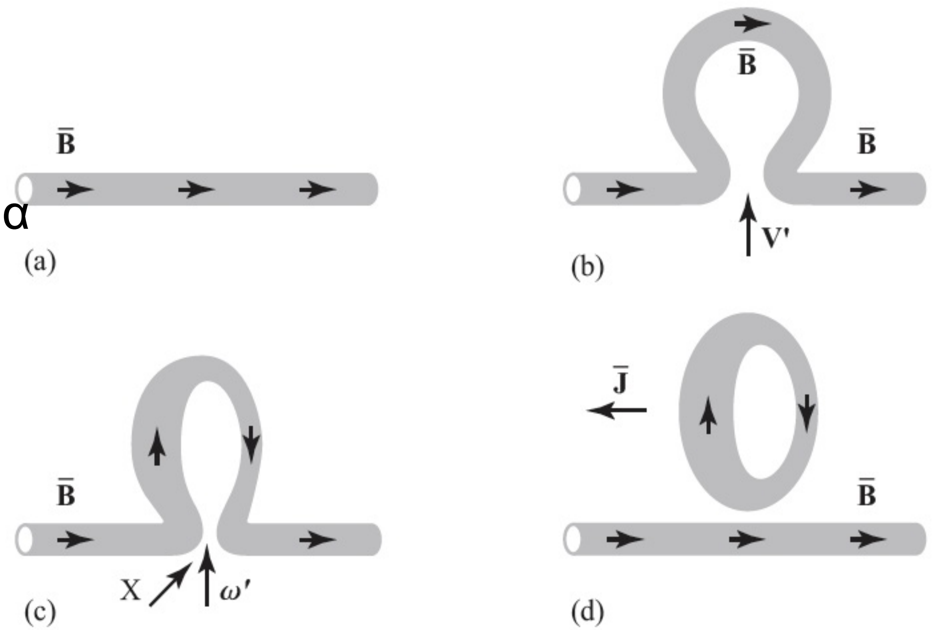

α

The cyclonic event mechanism as envisaged by Parker (after Roberts, 1994). The uniform field in (a) is pulled up in (b), twisted in (c), and then reconnects to form a field loop with a normal component (and so EMF) anti-parallel to the original field (d).

α effect (Parker) induced by an helical velocity field

Dynamo types

$\alpha\omega$ dynamo

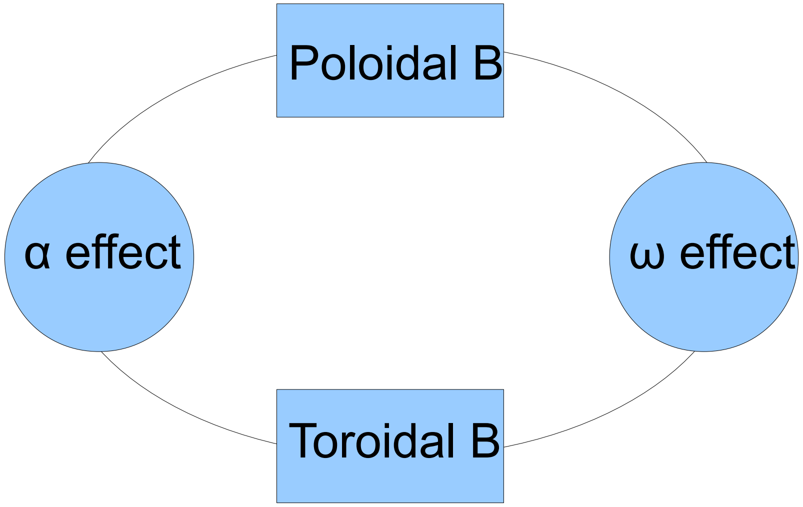

Oscillatory dynamos !?

α^2 dynamo

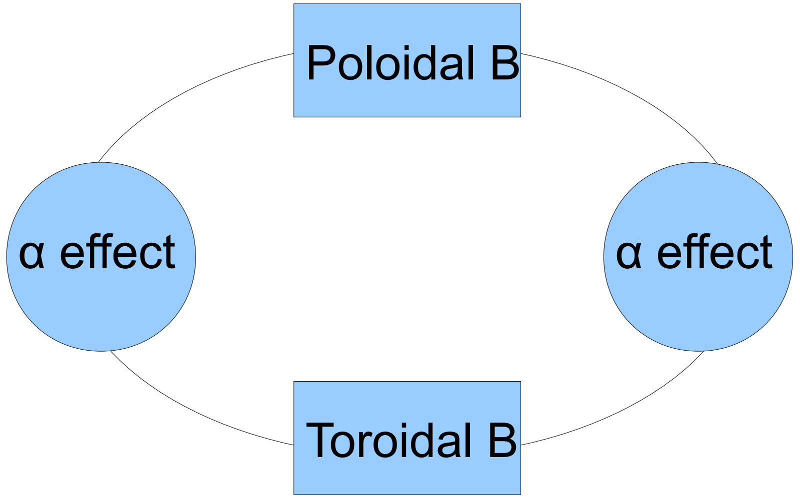

Stationary dynamos !?

Natural candidates for the MRI: Accretion Disks

Planet and Stellar Formation

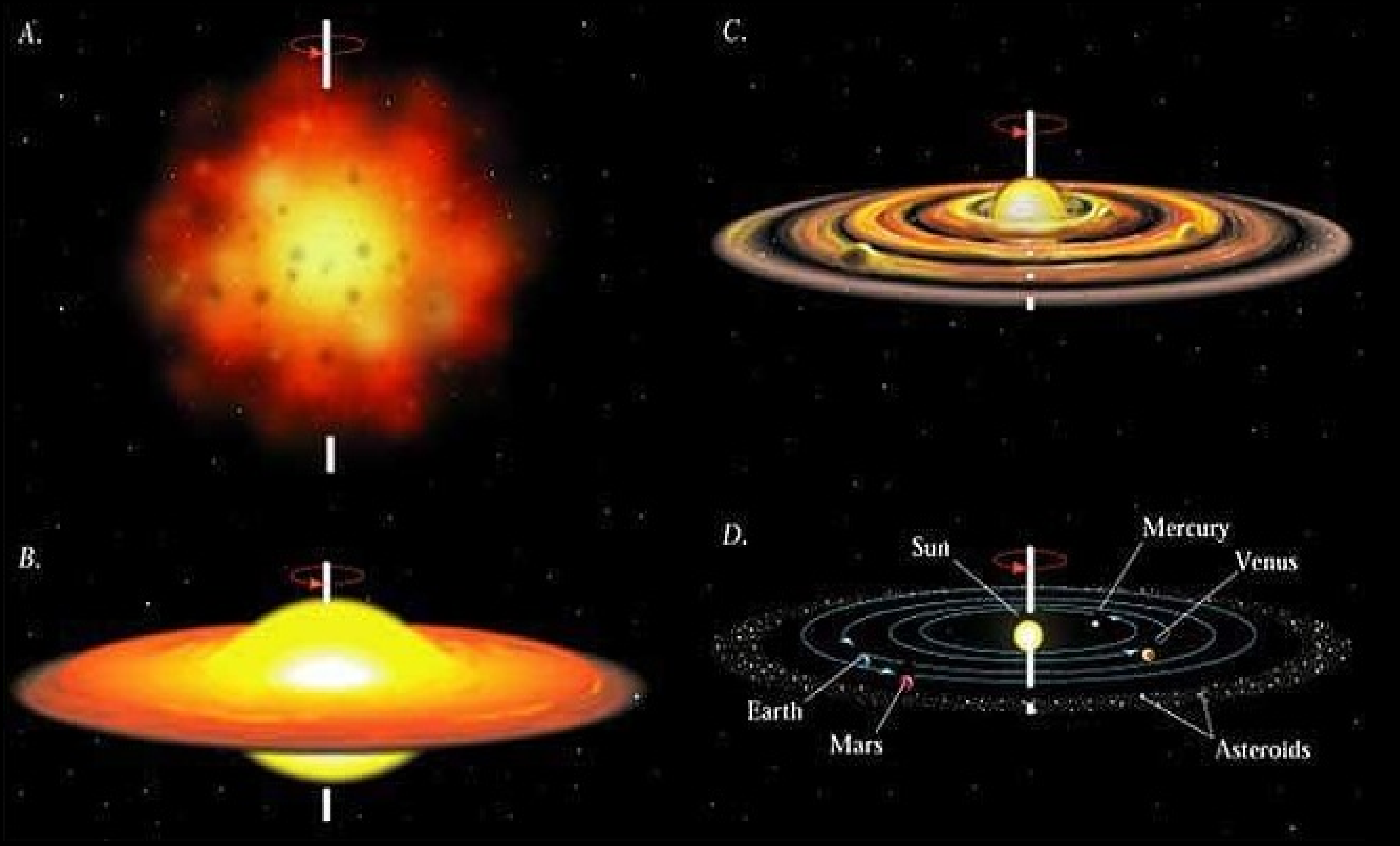

MRI triggers turbulence which allows accretion process

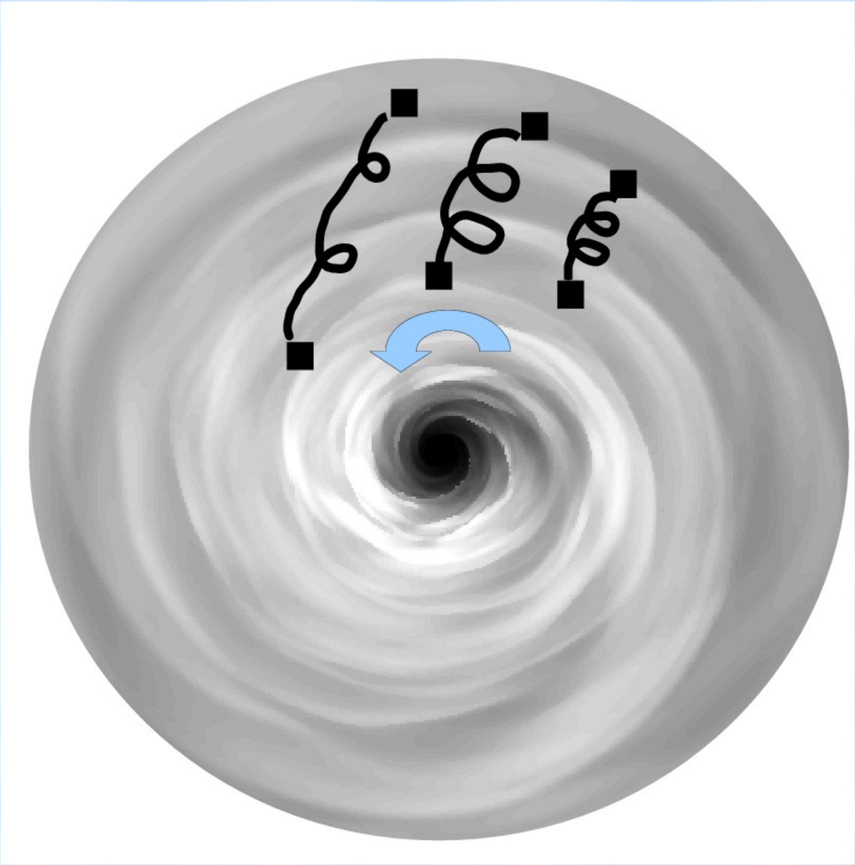

Reference state

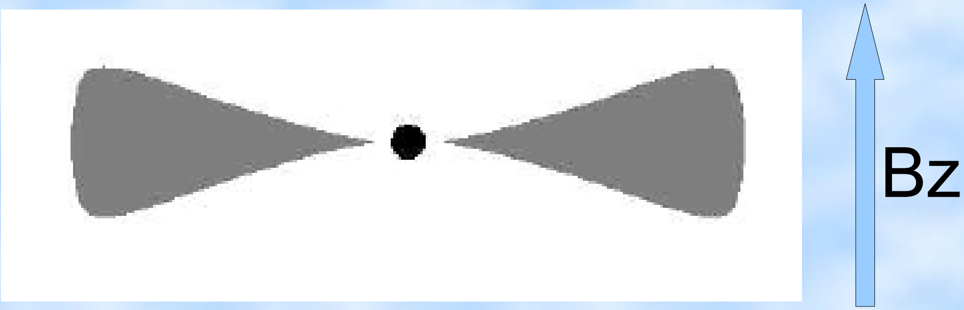

Keplerian rotation rate

$$\Omega^2 = \frac{GM}{R^3},$$

Dynamo process in accretion disks

- Cyclic time variations observed in local and global models

By (azimuthal average)

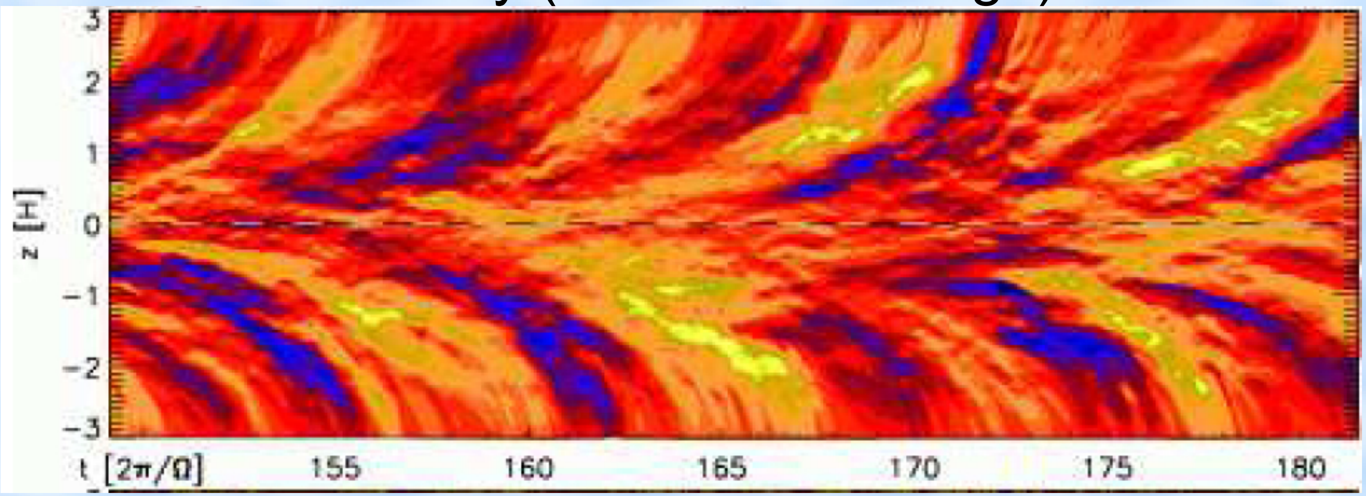

Gressel 2010

Dynamo process in accretion disks

- Cyclic time variations observed in local and global models
- Dynamo could provide large-scale poloidal field which allows MRI (Beckwith *et al* 2011)
  - Correlation observed between poloidal magnetic flux and Maxwell stress.
  - Dynamo affects the level of angular momentum transport.
- Convergence issue in local simulations if Pm<2
  - Without a net vertical magnetic flux: for small Pm, dynamo action is harder to excite.

From the Earth to the stars…

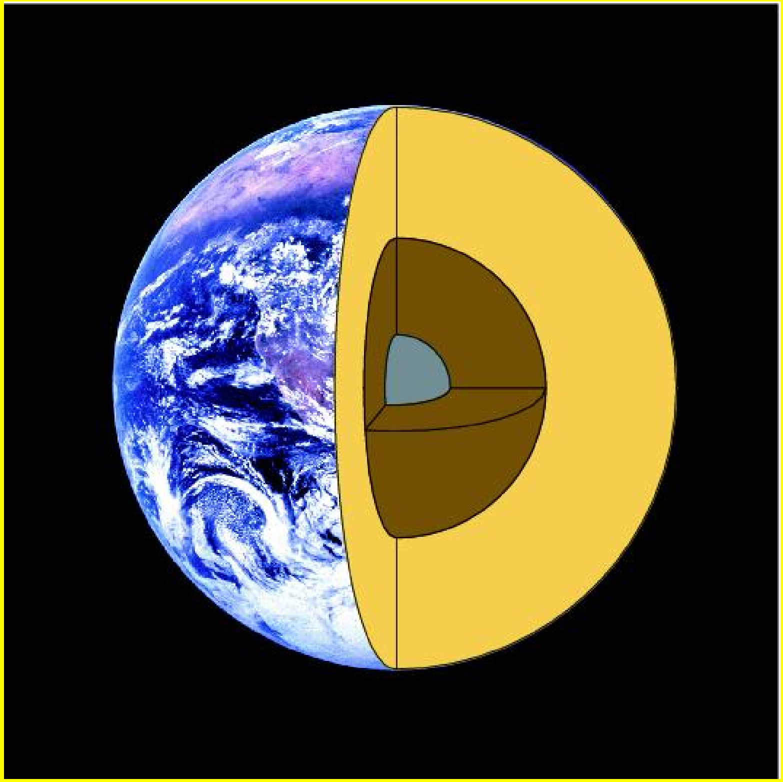

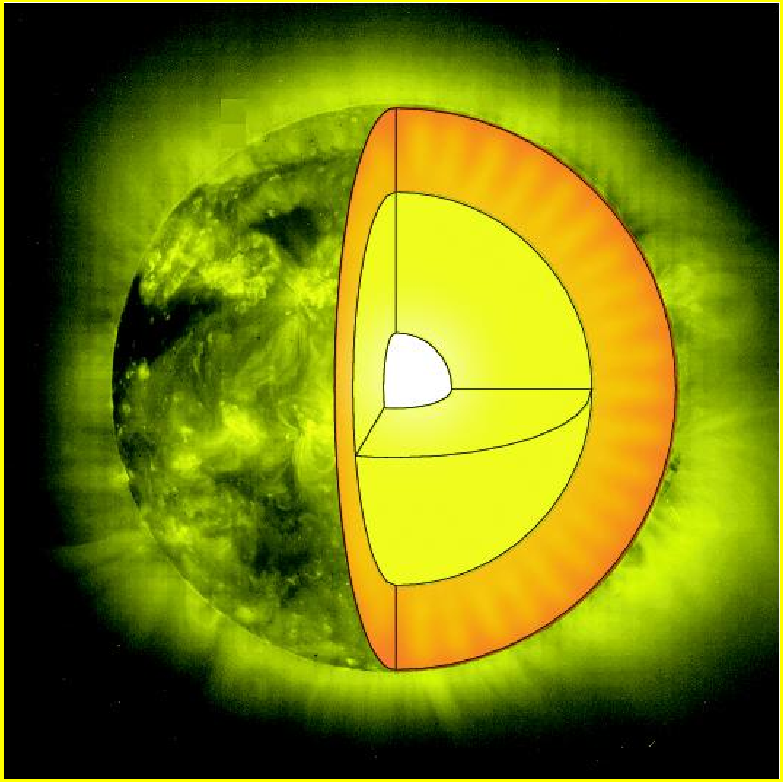

(Goudard & Dormy, EPL, **83**, 59001, 2008)

Dynamo Models

• Conducting Boussinesq fluid in a rotating spherical shell

• Convection driven by temperature gradient between inner and outer shell

• Aspect ratio: r_i/r_o

• MHD-code:

Parody (Dormy et al. 1998)

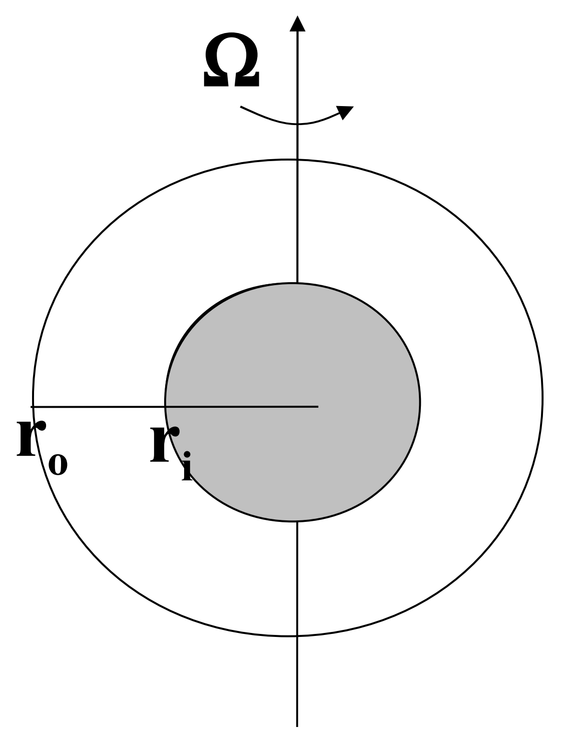

•Mixte mechanical boundary conditions: Rigid/Stress-Free

MHD-Equations (Boussinesq)

$$
\begin{aligned}
E\left(\frac{\partial \boldsymbol{V}}{\partial t} + \boldsymbol{V}\cdot\nabla\boldsymbol{V} - \nabla^2\boldsymbol{V}\right) + 2\hat{z}\times\boldsymbol{V} + \nabla P &= Ra\frac{\boldsymbol{r}}{r_o}T + \frac{1}{Pm}(\nabla\times\boldsymbol{B})\times\boldsymbol{B} \\
\nabla\cdot\boldsymbol{V} &= 0 \\
\frac{\partial T}{\partial t} + \boldsymbol{V}\cdot\nabla T &= \frac{1}{Pr}\nabla^2 T \\
\frac{\partial \boldsymbol{B}}{\partial t} &= \nabla\times(\boldsymbol{V}\times\boldsymbol{B}) + \frac{1}{Pm}\nabla^2\boldsymbol{B} \\
\nabla\cdot\boldsymbol{B} &= 0
\end{aligned}
$$

Solver: (Pseudo-)Spectral code, developed by Glatzmaier (1984), used here in the Version of Christensen et al. (1999)

PARODY, Dormy et al. (1998)

Two distinct regimes in geodynamo models

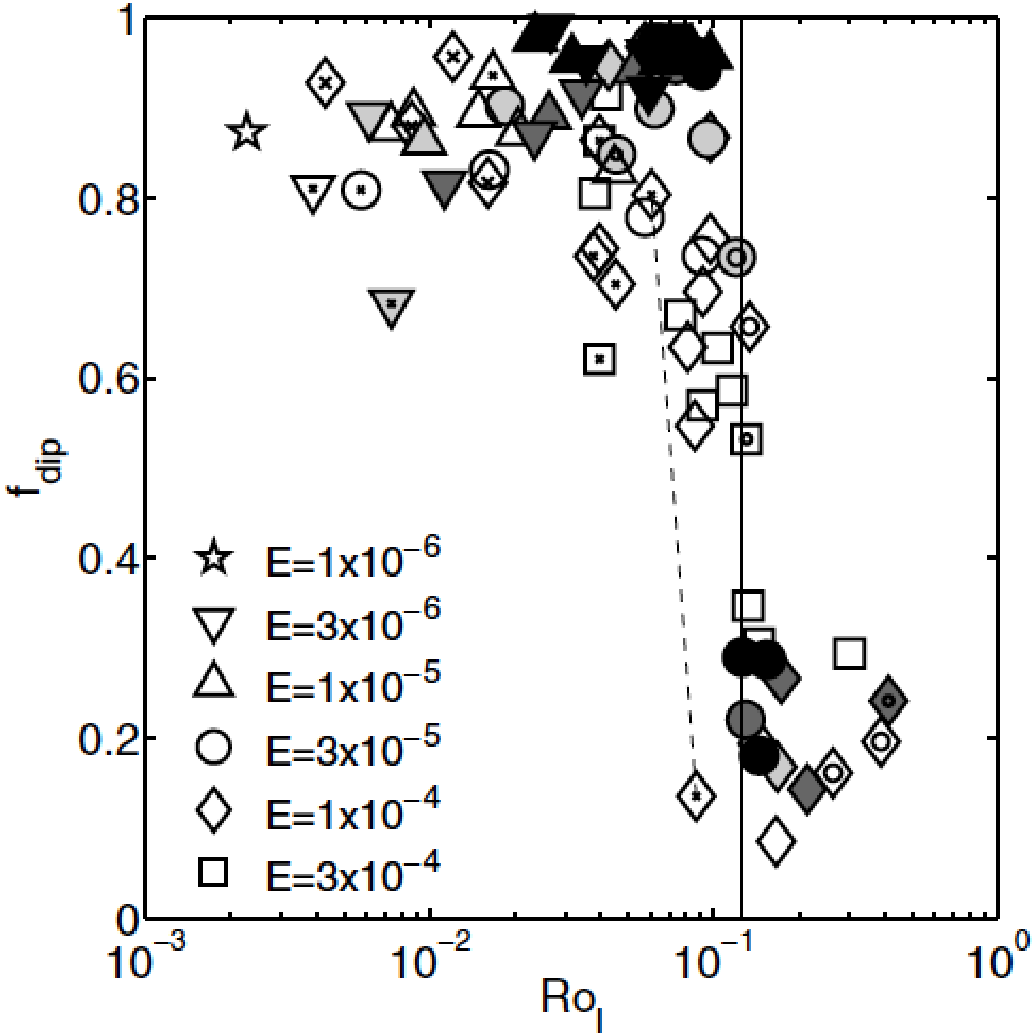

Christensen & Aubert, 2006

$$\bar{\ell}_u = \frac{\sum \ell \langle \mathbf{u}_\ell \cdot \mathbf{u}_\ell \rangle}{2E_{\mathrm{kin}}},$$

$$Ro_\ell = Ro\frac{\bar{\ell}_u}{\pi}.$$

Ro=V/(ΩL)= « inertial/Coriolis »

Dipole field strenght f_{dip}: time-average ratio on the outer shell boudary of the mean dipole field strength to the field strength in harmonic degrees l=1-12.

Fixed parameter set:

$$\mathrm{E} = \frac{\nu}{\Omega D^2}, \quad \widetilde{Ra} = \frac{\alpha g \Delta T D}{\nu \Omega}, \quad \mathrm{Pr} = \frac{\nu}{\kappa}, \quad \mathrm{Pm} = \frac{\nu}{\eta}.$$

$$\mathrm{E} = 10^{-3}, \;\; \widetilde{Ra} = 100,$$

$$\mathrm{Pr} = 1, \; \mathrm{Pm} = 5.$$

Impact of the Aspect ratio (Goudard & Dormy 2008)

Time and azimuthal average
of the zonal flow

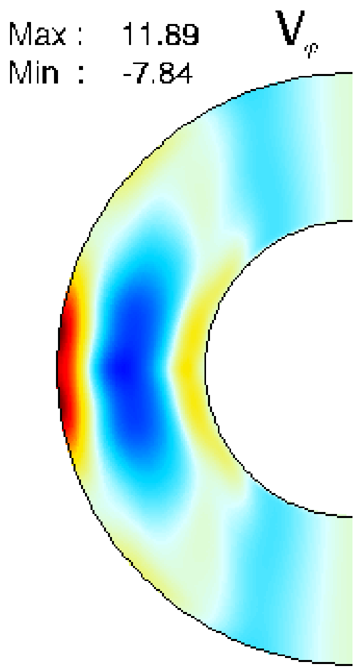

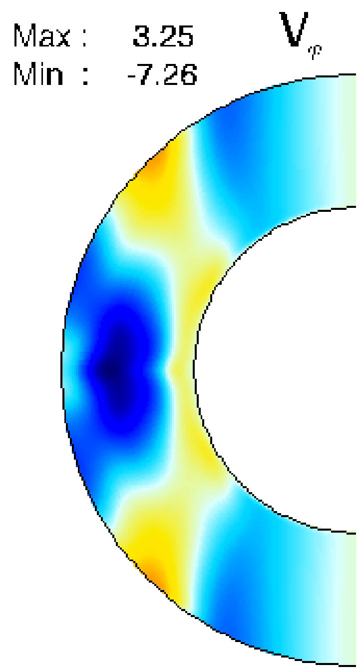

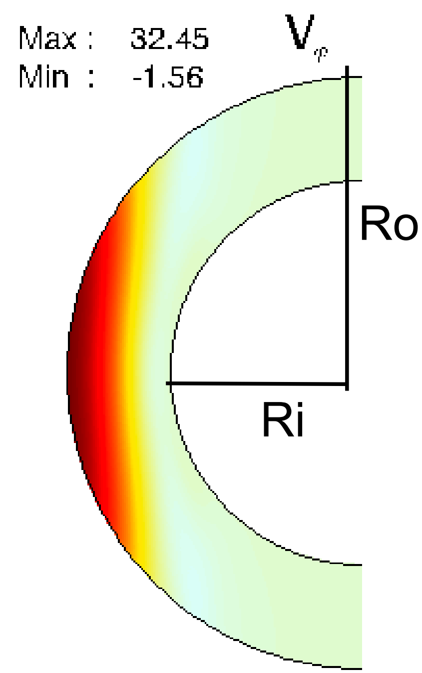

X=Ri/Ro=0.50

X=0.55

X=0.65

Stable dipolar dynamos

Oscillatory dynamo

The same Dynamo Models

- Conducting Boussinesq fluid in a rotating spherical shell
- Convection driven by temperature gradient between inner and outer shell
- Aspect ratio: r_i/r_o
- MHD-code:

Parody (Dormy et al. 1998)

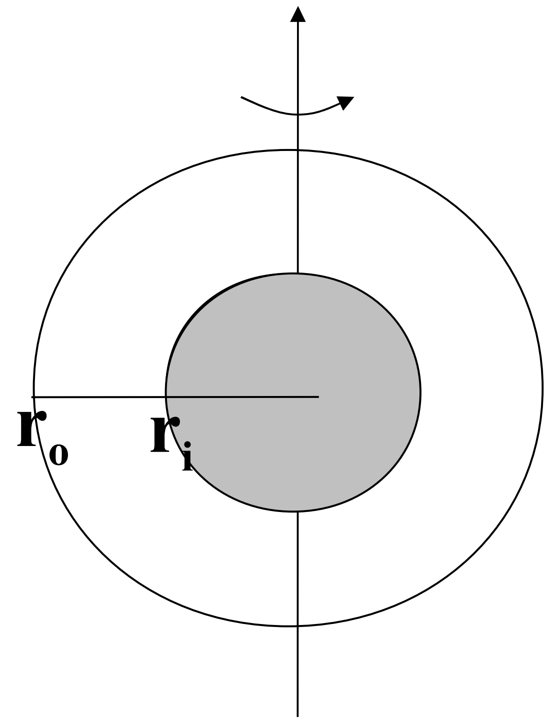

- We determine dynamo coefficients
- Tracer field equations without ω effect

$$\frac{\partial \boldsymbol{B}_{\mathrm{Tr}}}{\partial t} = \nabla \times (\boldsymbol{v} \times \boldsymbol{B}_{\mathrm{Tr}}) + \frac{1}{Pm} \nabla^2 \boldsymbol{B}_{\mathrm{Tr}} - \nabla \times \left(\overline{\boldsymbol{V}} \times \overline{\boldsymbol{B}}_{\mathrm{Tr}} \right),$$

Transition:
Dipolar stationary dynamos to oscillatory dynamos

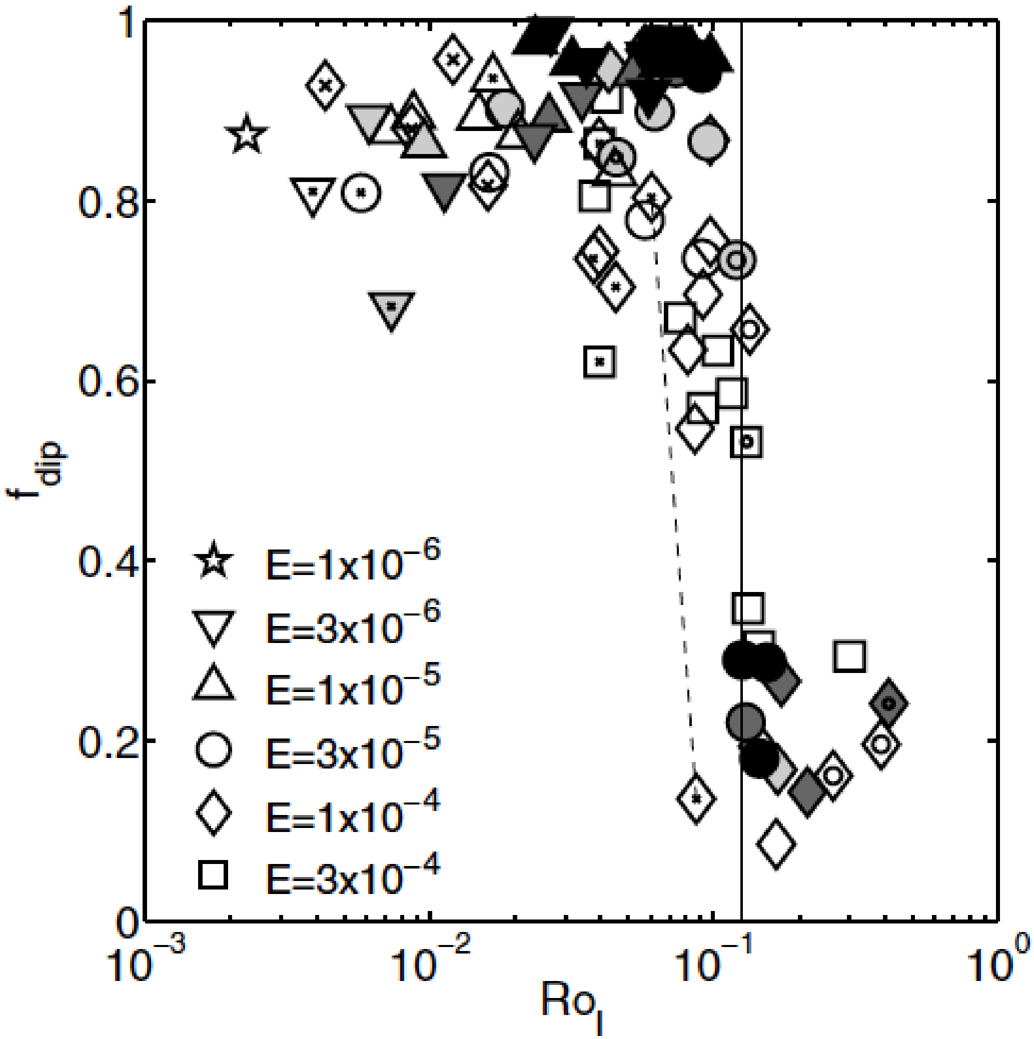

Geodynamos simulations
using different dimensionless parameters

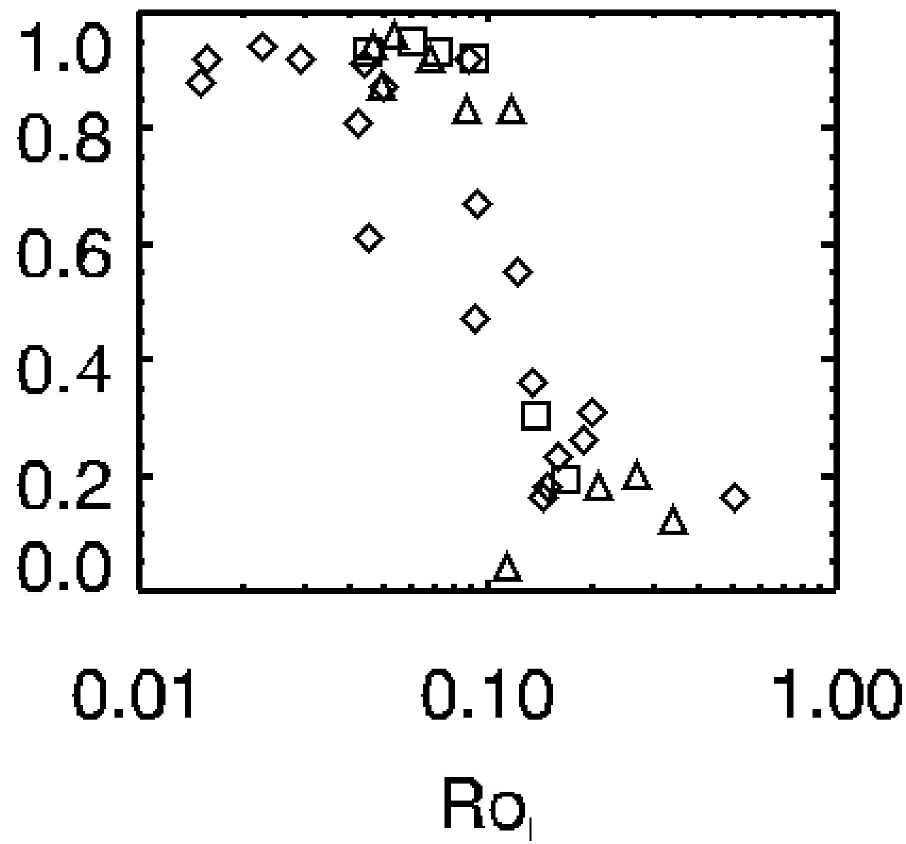

Boundary conditions
Δ Rigid/Stress-Free
□ Stess-Freed/Stress-Free
◊ Rigid/Rigid

Test-field method

- Perform MHD-simulation.
- « Measure » the mean electromotive force $\mathcal{E}$ generated by the action of the velocity field on certain test-fields.
- Extract coefficients out of expansion of $\mathcal{E}$,

$$\mathcal{E}_{\kappa}^{(i)} = \alpha_{\kappa\lambda} B_{T\lambda} + \beta_{\kappa\lambda\mu} \frac{\partial B_{T\lambda}}{\partial x_{\mu}}$$

Schrinner et al. 2005, 2007

Brandenburg, Rädler, Schrinner 2008

Tilgner, Brandenburg 2008

Rädler, Brandenburg 2009

…

Eigenvalue Problem

$$\begin{aligned} \lambda \boldsymbol{B} &= \nabla \times D\boldsymbol{B} \\ D\boldsymbol{B} &= \boldsymbol{u} \times \boldsymbol{B} - \eta \nabla \times \boldsymbol{B} \end{aligned}$$

Averaging in azimuth:

$$D\boldsymbol{B} = \boldsymbol{V} \times \boldsymbol{B} + \boldsymbol{\alpha} \cdot \boldsymbol{B} - \boldsymbol{\beta} : \nabla(\boldsymbol{B}) - \eta \nabla \times \boldsymbol{B}$$

α,β : Tensors of second and third rank respectively, depending on the velocity field.

They are determined with the help of the test-field method.

(e.g. Schrinner et al. 2005, 2007, Schrinner et al. 2010)

Direct numerical simulation

Leading eigenmode

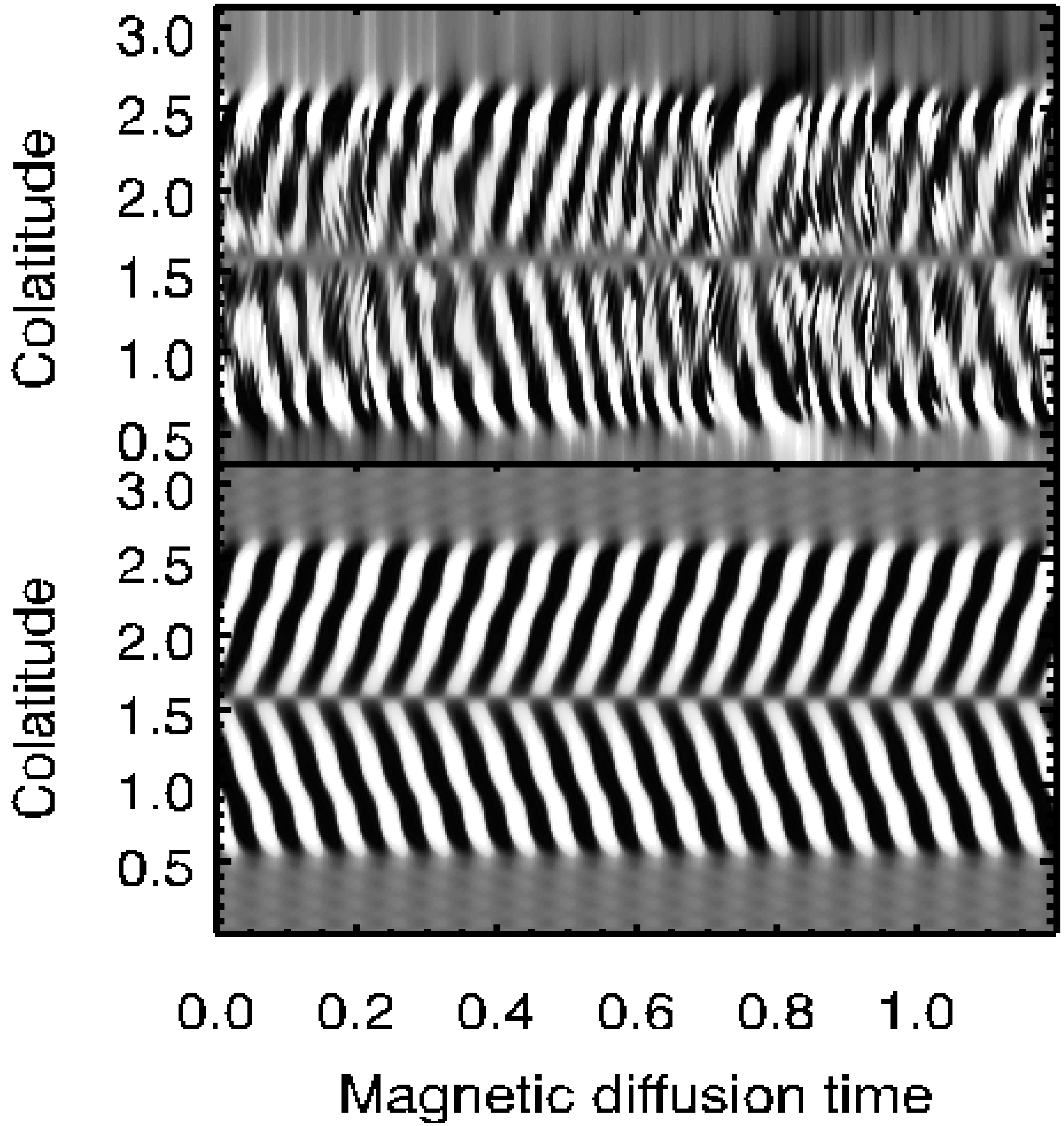

Schrinner, Petitdemange, Dormy, A&A (2011)

Dynamo mechanism

Tracer field without omega-effect

Eigenmode (for α^2)

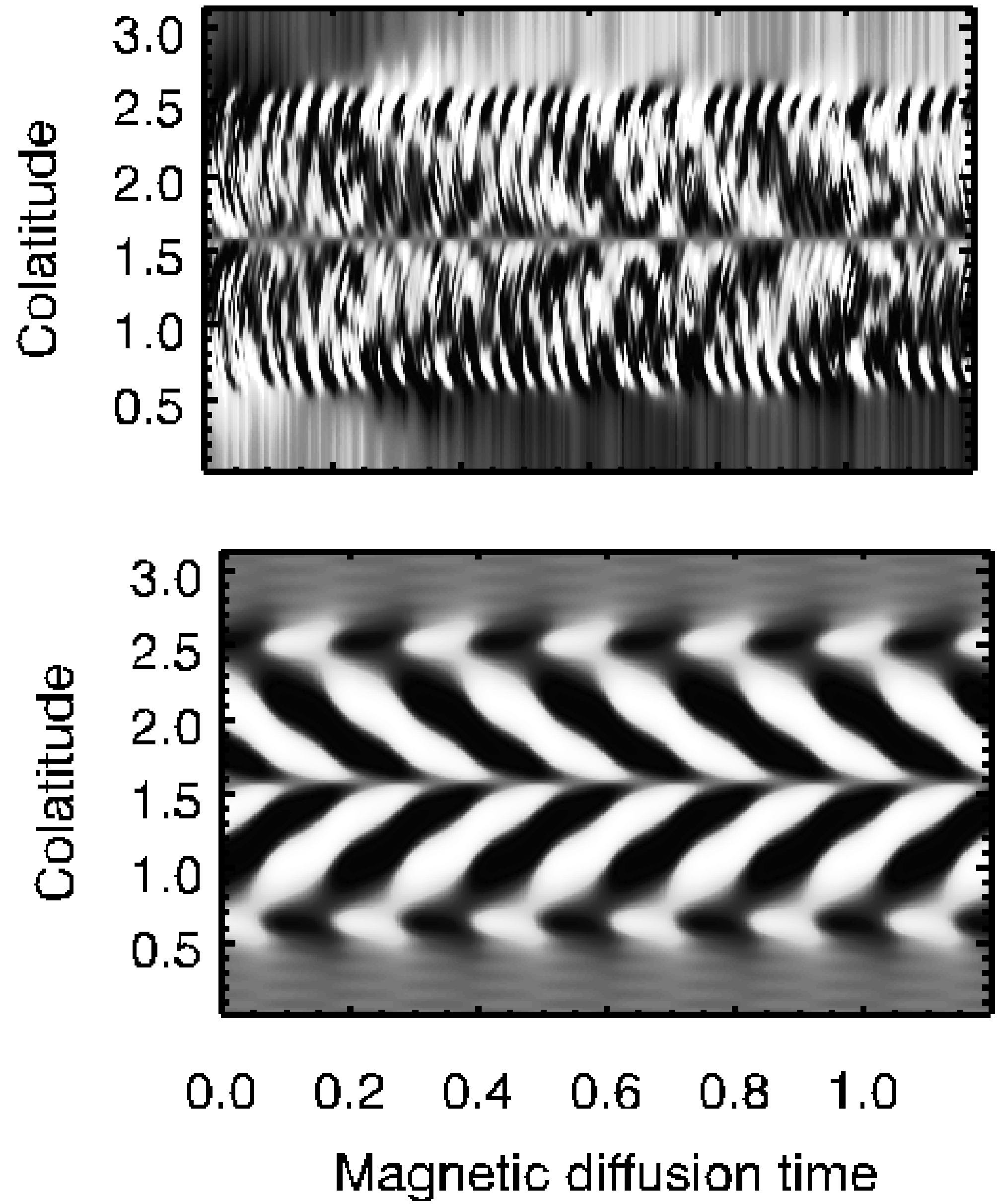

Results

- The transition is still caused by small scale convective motions.
- This oscillatory dynamo is of $\alpha^2\omega$ type:
  - α^2 dynamo is also oscillatory

    Differential rotation alone is not responsible for oscillatory behavior
  - $\alpha\omega$ Dynamo is dipolar and stationary !
- We use the same method in order to understand bistability in numerical models with stress-free mechanical Boundary conditions.

The same Dynamo Models

- Conducting Boussinesq fluid in a rotating spherical shell
- Convection driven by temperature gradient between inner and outer shell
- Aspect ratio=0.35: $r_i/r_{o=}$
- MHD-code:

Parody (Dormy et al. 1998)

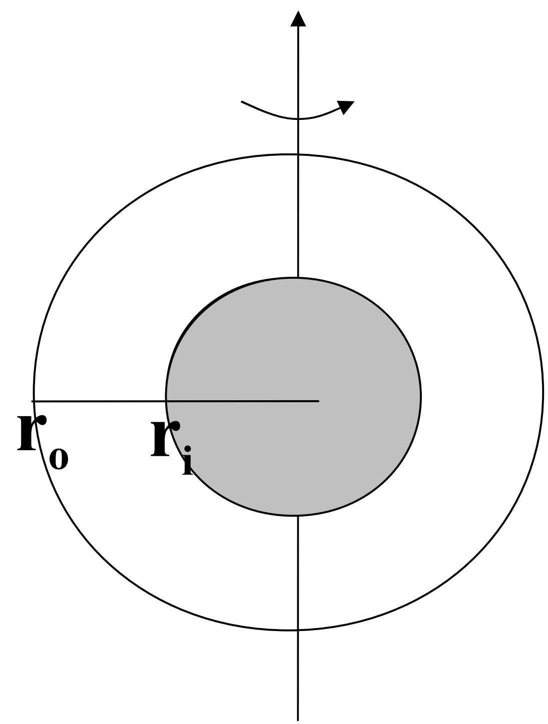

- Stress-Free boundary conditions
- Two distinct regime obtained for different initial conditions

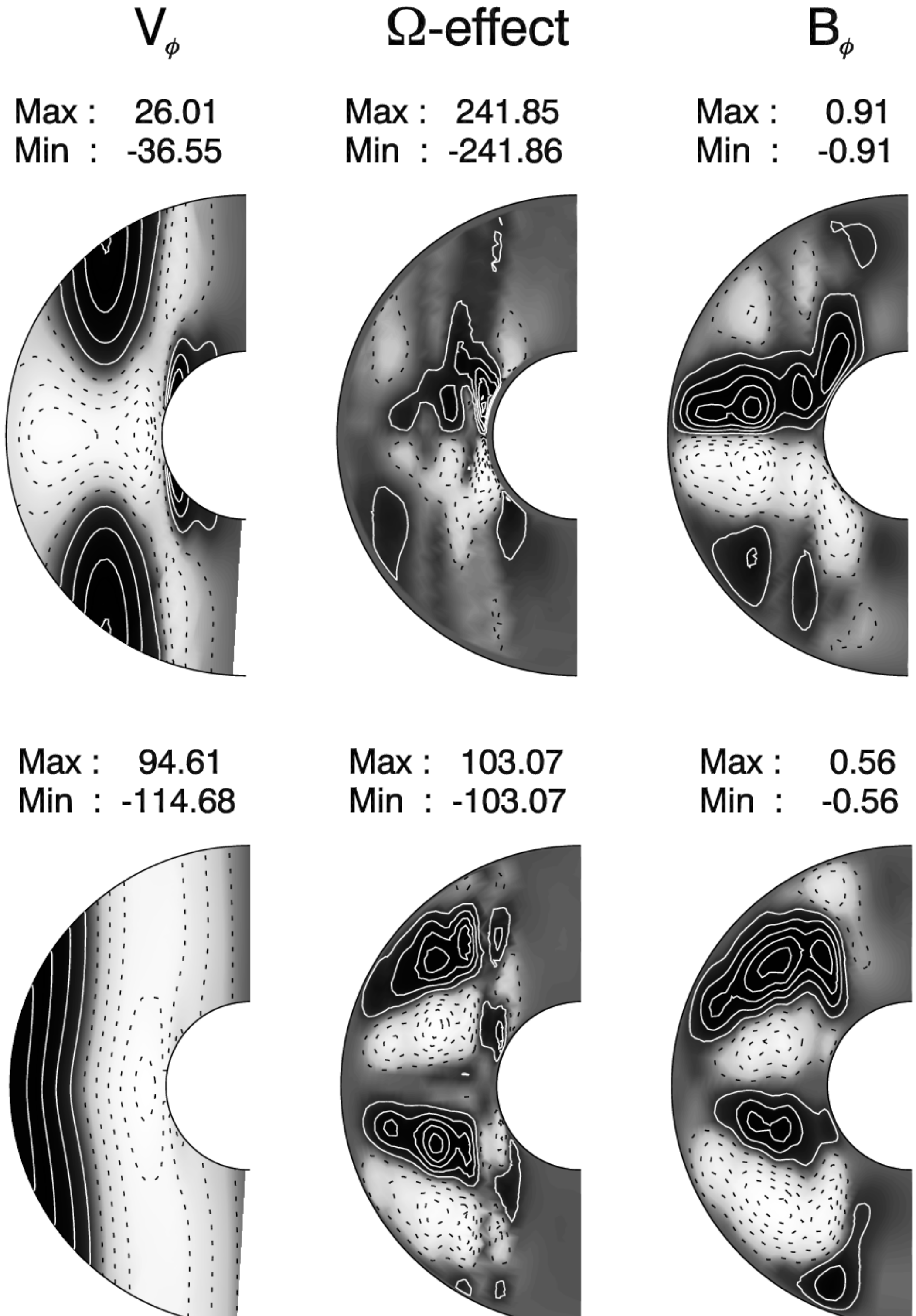

Strong field branch

Dipolar and stationary

Weak fild branch

Oscillatory dynamos

Schrinner, Petitdemange, Dormy (2011b)
In prepartion

Bistability induced by large-scales differential rotation

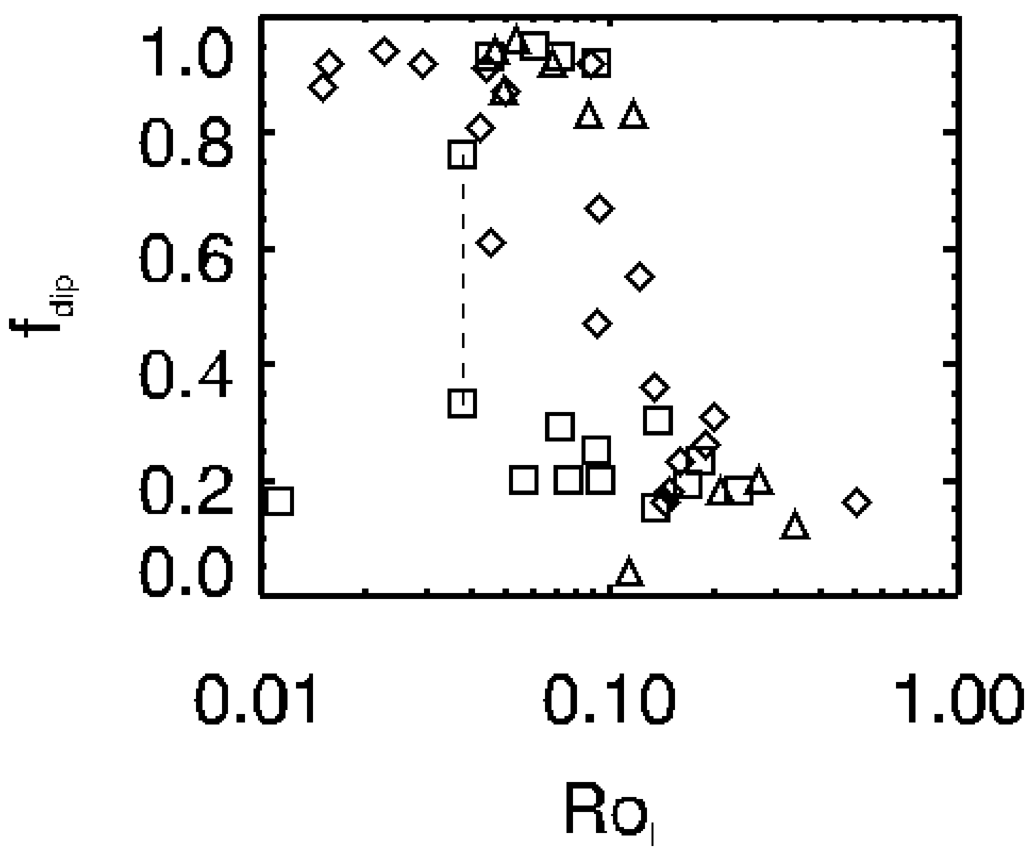

Boundary conditions

Δ Rigid/Stress-Free
□ Stess-Freed/Stress-Free
◊ Rigid/Rigid

A model for stellar dynamos ?

- Weak/strong field branches could explain bistability

- Problems with butterfly diagram
  - Towards poles rather than the equator.
  - If Rm>250, no coherent butterfly diagrams

- Aditional physical processes are needed:
  - Compressible effects, tachocline...
  - Parameter regime allowing MRI modes.

MRI and planetary interiors

Using simple models of planetary interiors

Rapidly rotating systems

Geostrophic balance

$$2\Omega \mathbf{e_z} \times \mathbf{u} = -\nabla \pi$$

Proudman-Taylor Theorem:

$$\frac{\partial \mathbf{u}}{\partial z} = \mathbf{0}$$

Magnetostrophic balance

$$2\Omega \mathbf{e_z} \times \mathbf{u} = -\nabla \pi + \frac{\mathbf{1}}{\mu_0 \rho_0} (\nabla \times \mathbf{B}) \times \mathbf{B}$$

$$R_o = \frac{\Delta \Omega}{\Omega} \ll 1$$

Angular velocity

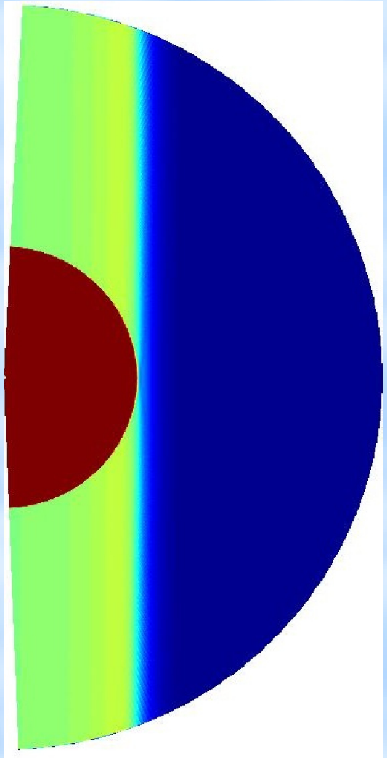

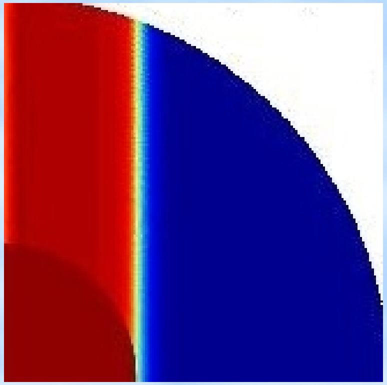

MHD stationnary solution with only vertical B field

Local Description

$$2\boldsymbol{\Omega} \times \boldsymbol{V} = -\nabla\Pi + \frac{1}{\mu\rho}(\boldsymbol{B}\cdot\nabla)\boldsymbol{B},$$

$$\left(\frac{\partial}{\partial t} + \boldsymbol{V}\cdot\nabla\right)\boldsymbol{B} = (\boldsymbol{B}\cdot\nabla)\boldsymbol{V} + \eta\nabla^2\boldsymbol{B}.$$

$$Q \propto \exp(ik_s s + ik_z z + \sigma t)$$

$$-2\Omega v_\phi = \frac{ikB_0}{\mu_0\rho} b_s,$$

$$2\Omega v_s = \frac{ikB_0}{\mu_0\rho} b_\phi.$$

$$(\sigma + \eta k^2) b_s = ikB_0 v_s,$$

$$(\sigma + \eta k^2) b_\phi = ikB_0 v_\phi + s\frac{d\Omega}{ds} b_s.$$

The Instability Mechanism

$$(\sigma + \eta k^2) b_\phi = \left[\frac{(kV_A)^2}{2\Omega} + s \frac{d\Omega}{ds} \right] b_s .$$

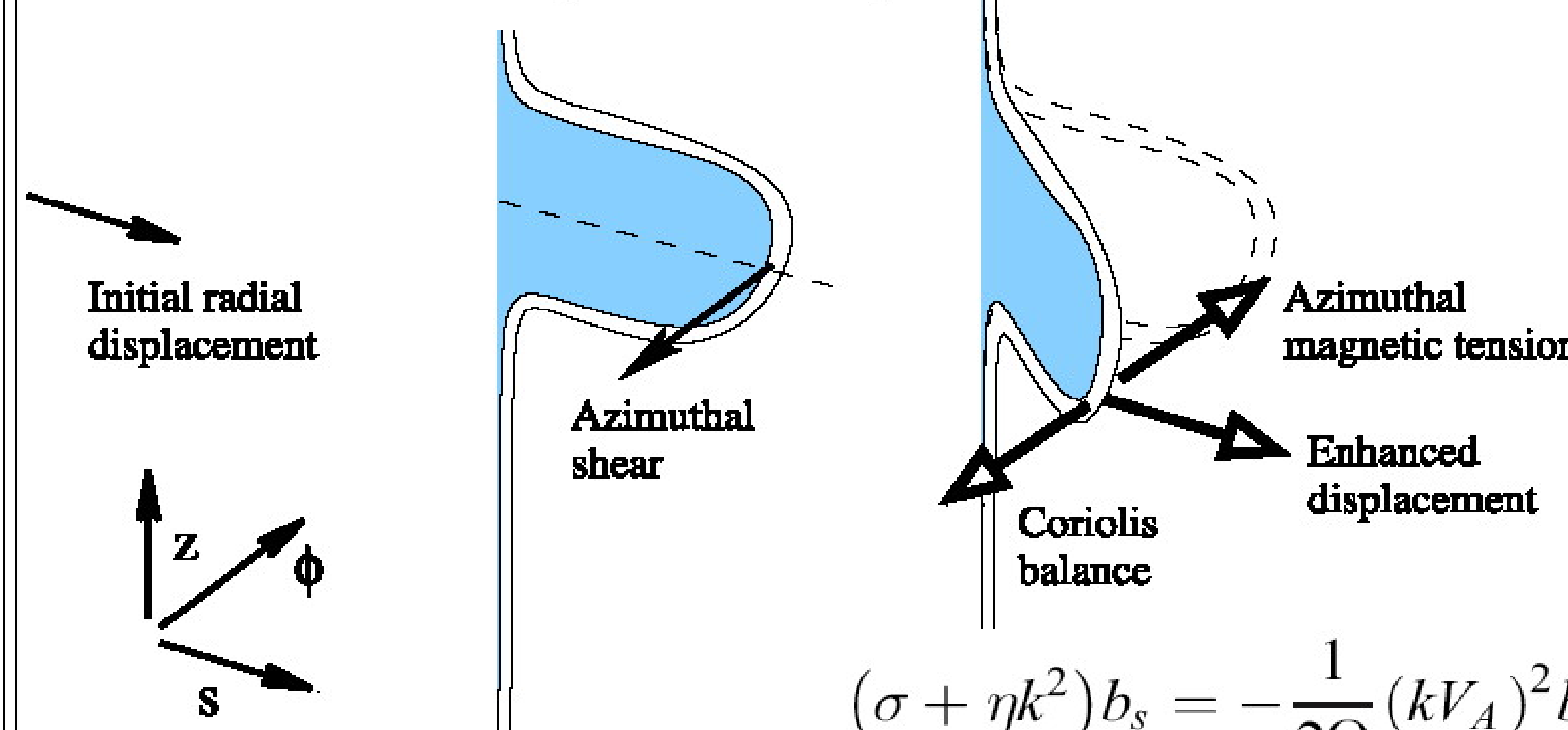

$$(\sigma + \eta k^2) b_s = -\frac{1}{2\Omega} (kV_A)^2 b_\phi ,$$

Dispersion Relation

$$(kV_A)^4 + 4\Omega^2(\sigma + \eta k^2)^2 + (kV_A)^2 s \frac{d\Omega^2}{ds} = 0,$$

$$\sigma = \left| s \frac{d\Omega}{ds} \right| \frac{\Lambda/2}{1 + \sqrt{1 + \Lambda^2}}.$$

Elsasser number

$$\Lambda = \frac{V_A^2}{2\eta\Omega_0} = \frac{B_0^2}{2\mu_0 \rho \eta \Omega_0},$$

MS-MRI could explain time variations
From 1 year to 10000 years.

Direct Linear Numerical Simulations (DNS)

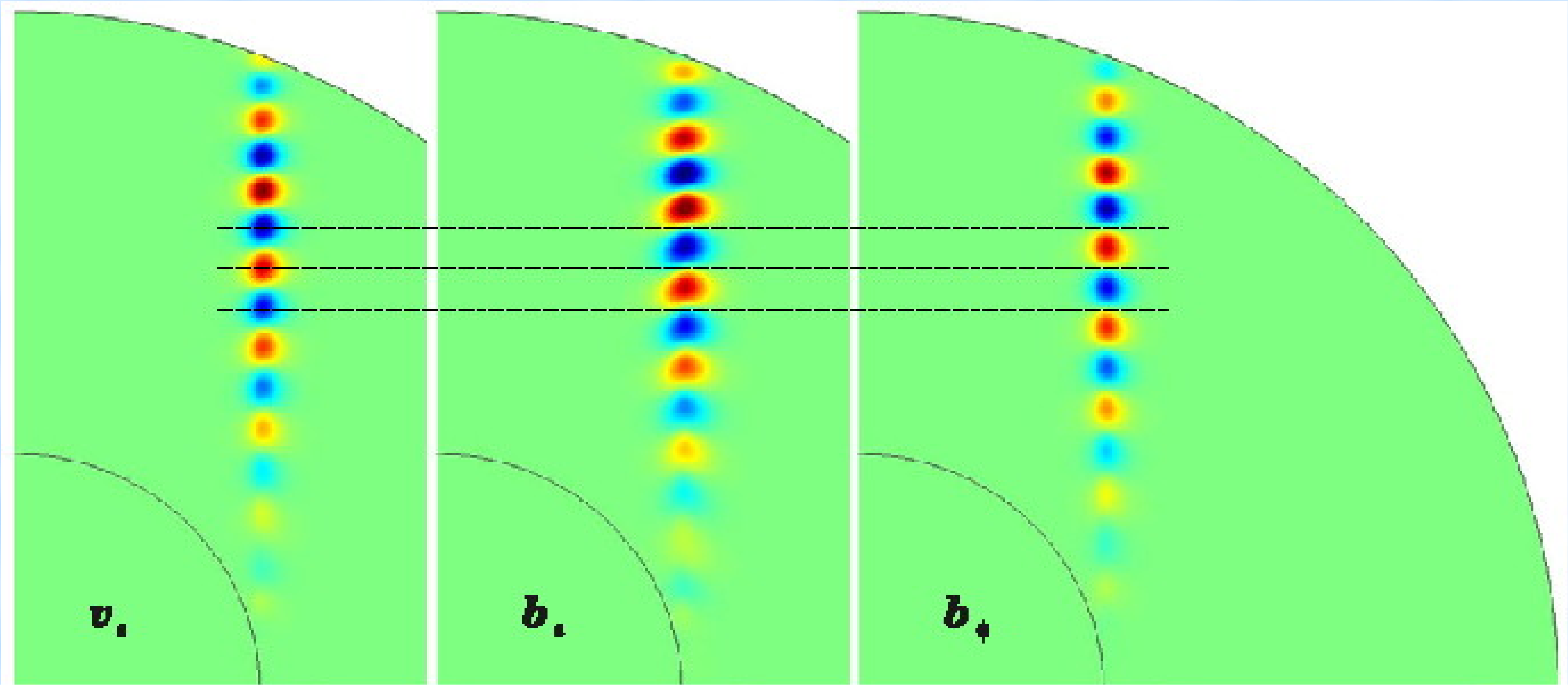

$E = \frac{\nu}{2\Omega_0 r_o^2}$	Λ	R_o	growht rate $(T = \frac{1}{\Omega})$	num growth rate
$2.5.10^{-7}$	0.5	0.005	$2.06.10^{-3}$	$1.84.10^{-3}$

L.Petitdemange, E.Dormy, S.Balbus, GRL (2008)

Axisymmetric Non-linear Developments

L. Petitdemange, GAFD, (2010).

Saturation of the MS-MRI

Angular velocity (z-averaged)

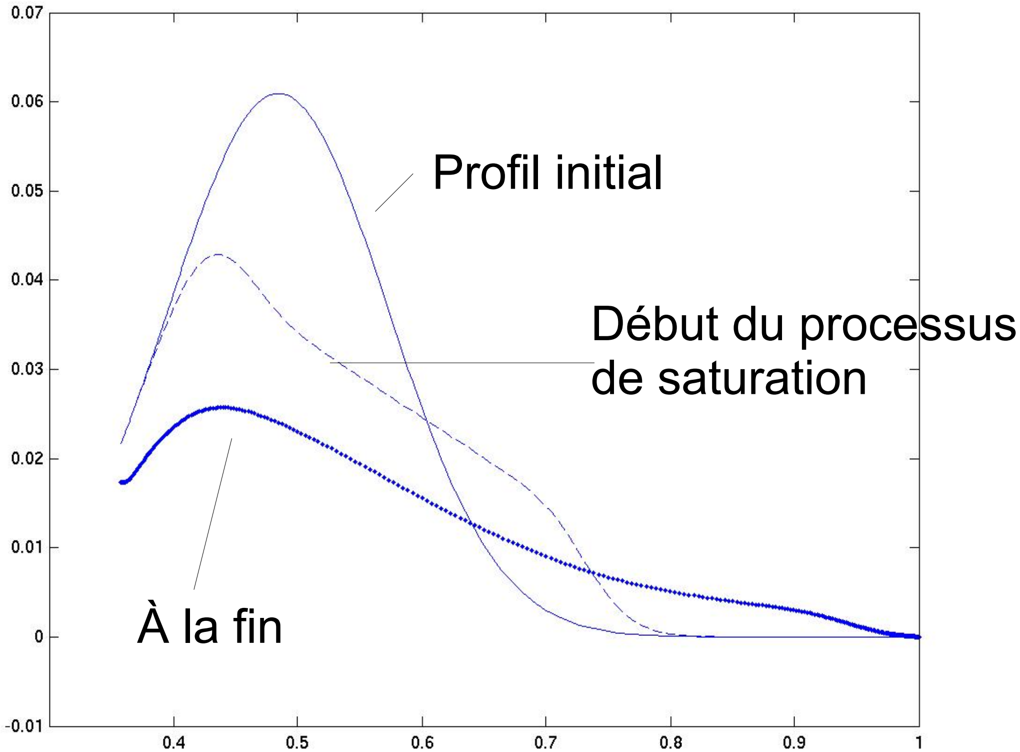

S: cylindrical radius

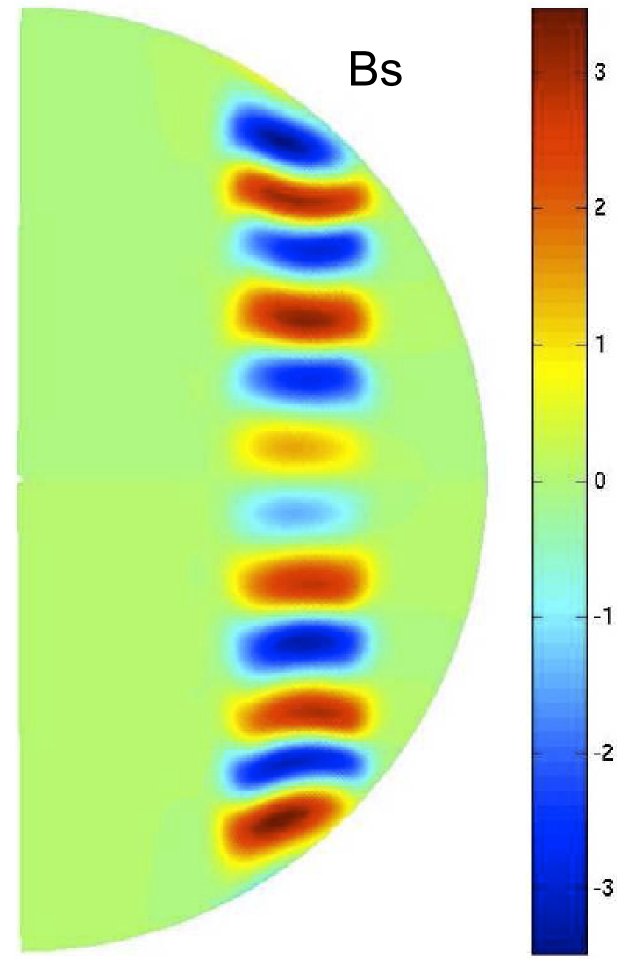

$$R'_o = \frac{d \ln \Omega}{d \ln s}$$ =0.062

3-D MS-MRI modes

without curvature terms

Local framework with background shear requires the use of shearing coordinates

$$\frac{d^2 b_s}{dt^2} + \frac{s}{2\Omega}\frac{d\Omega}{ds}(k \cdot V_A)^2 b_s + \frac{(k \cdot V_A)^4}{4\Omega^2}\frac{k_{tot}^2}{k_z^2} b_s$$

$$+ 2\eta k_{tot}^2 \frac{db_s}{dt} - 2\eta k_s \frac{m}{s} s\Omega' b_s + \eta^2 k_{tot}^4 b_s = 0$$

3-D MS-MRI modes (Bz)

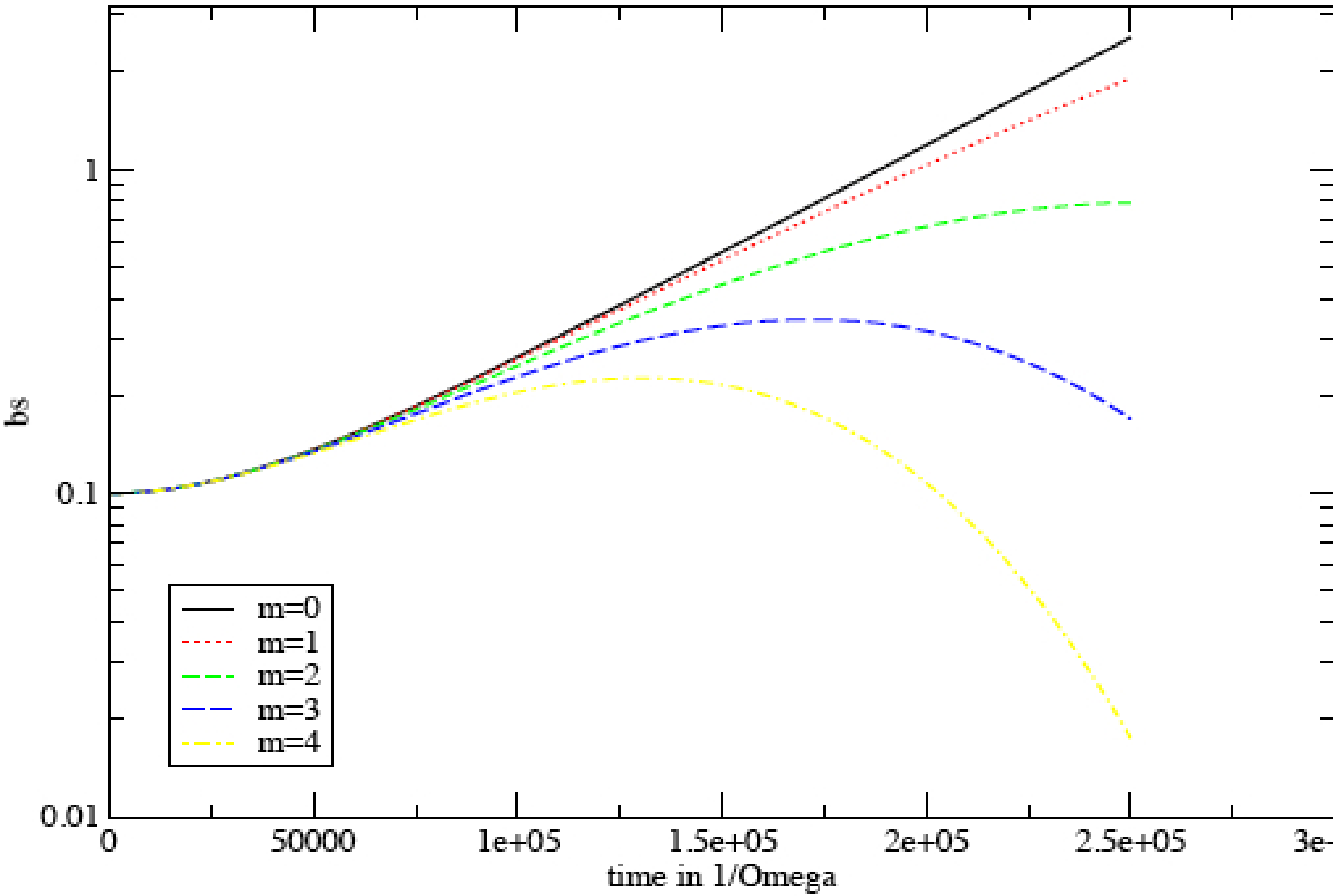

3-D MS-MRI modes ($\beta=B_\varphi/B_z=3$)

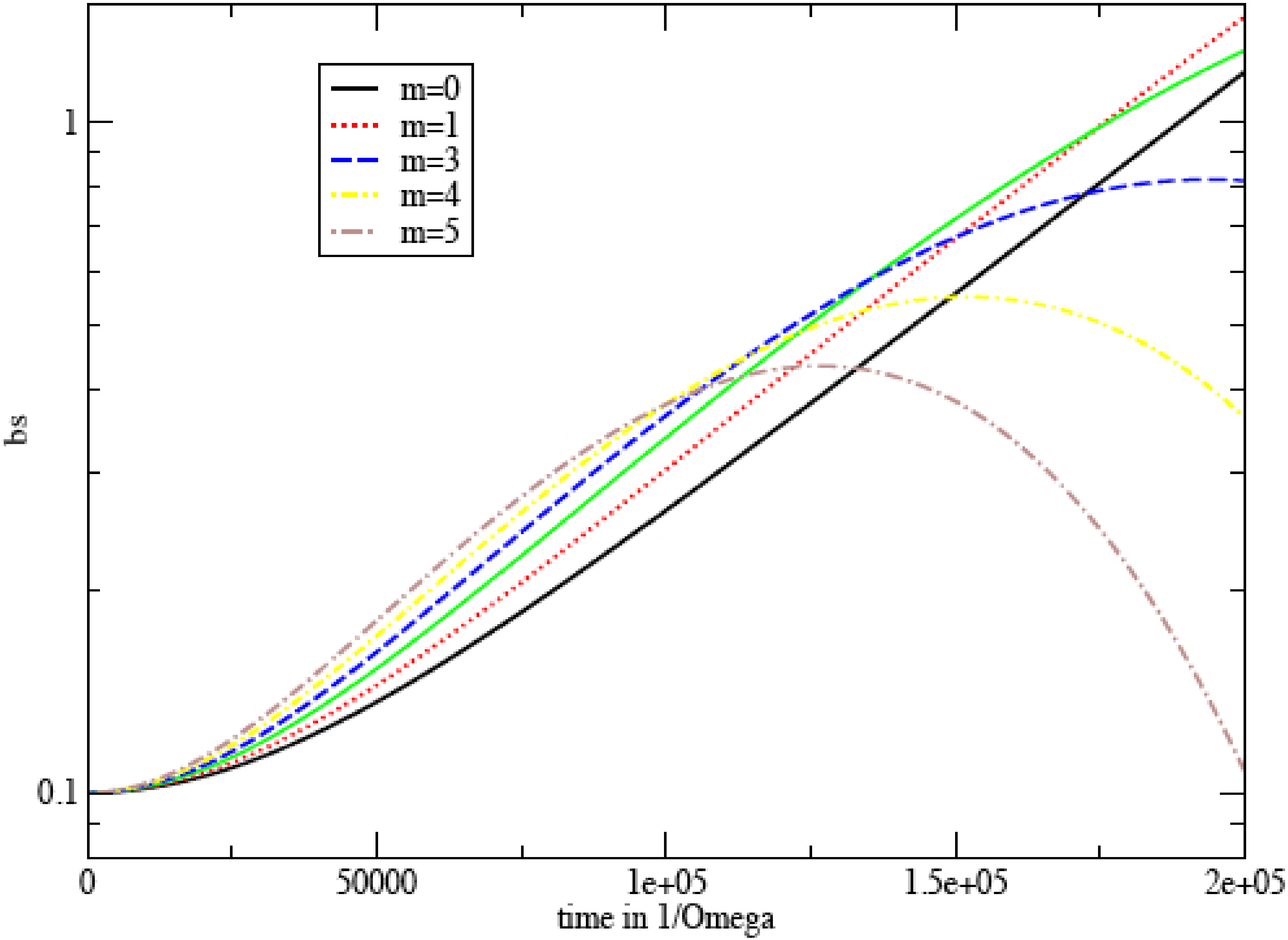

Helical background field on axisymmetric disturbances

- Linear DNS with background $B_\phi=2\beta s$ and B_z
  - Applied Lorentz force balanced by pressure gradient
  - Such a helical field avoids Acheson-type instability
- Local description: in considering curvature terms
  - It highlights the physical mechanism.
  - It is used for a direct comparison with DNS.
  - It allows to consider Planetary Interiors regime.
  - Any radial dependency for B_ϕ can be used.

Non-linear axisymmetric DNS

with an applied velocity Uo
and helical background B, β=10

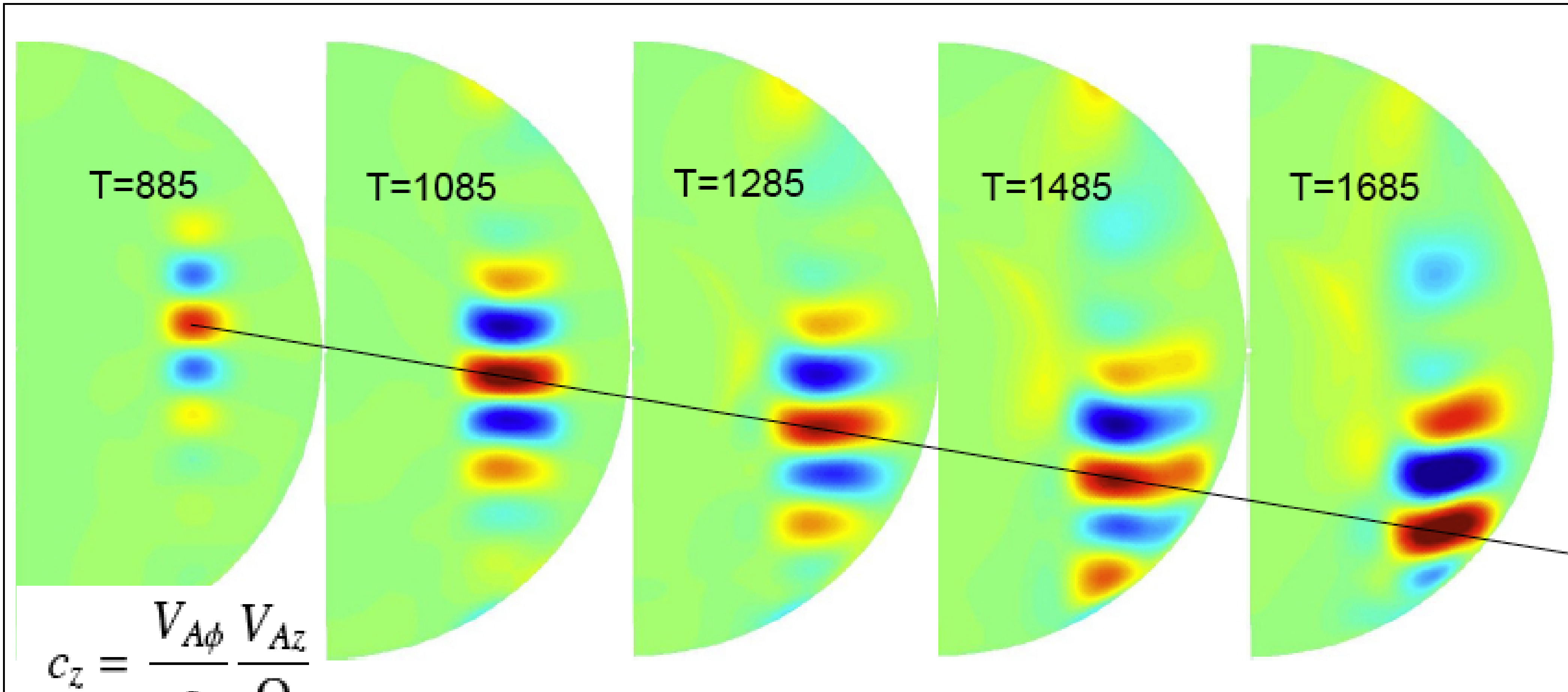

$$c_z = \frac{V_{A\phi}}{s}\frac{V_{Az}}{\Omega}$$

The wave paquet drifts at a fixed rate even if saturation occurs.

3-D MS-MRI modes

cylindrical shearing coordinates
(with curvature terms)

$$\frac{d^2 b_s}{dt^2} + \left(2\Omega\eta k_{tot}^2 - 2Fi\mathbf{k}\cdot\mathbf{V_A}\right)\frac{db_s}{dt} + \left(\eta k_{tot}^2 - \frac{Fi\mathbf{k}\cdot\mathbf{V_A}}{\Omega}\right)^2 b_s$$

$$+\frac{k_{tot}^2}{k_z^2}\frac{(\mathbf{k}\cdot\mathbf{V_A})^4}{4\Omega^2} b_s + (\mathbf{k}\cdot\mathbf{V_A})^2\frac{\mathbf{s}\boldsymbol{\Omega}'}{\mathbf{2}\boldsymbol{\Omega}}\mathbf{b_s} - \mathbf{2}\eta\mathbf{s}\boldsymbol{\Omega}'\frac{\mathbf{mk_s}}{\mathbf{s}}\mathbf{b_s} = \mathbf{0}\ .$$

$F = V_{A\Phi}/s$

From DNS:

m=3:

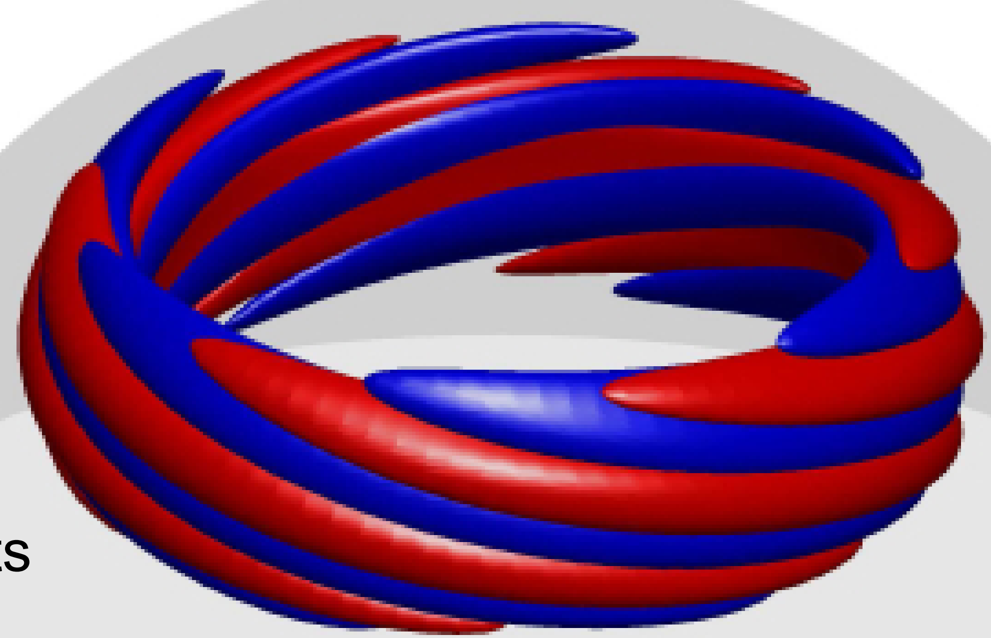

Numerical Results

Isosurface of
Kinetic (blue)
Magnetic (red)
energies

The MS-MRI and the magnetic gradient instability

(Acheson & Hide 1973, Fearn 1994)

Instability criteria:

$$\frac{d}{ds}\left(\frac{B_\phi^2}{s^2}\right) > \Delta_c(B_\phi, \eta)$$

Non-linear DNS

Angular velocity

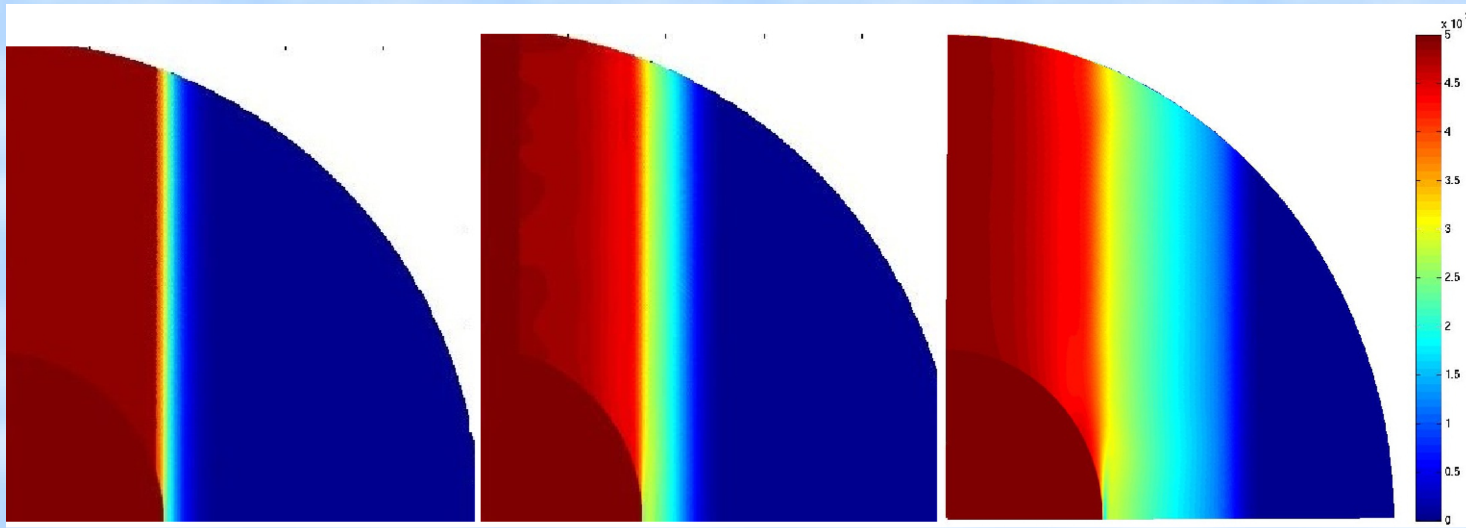

Azimuthal field

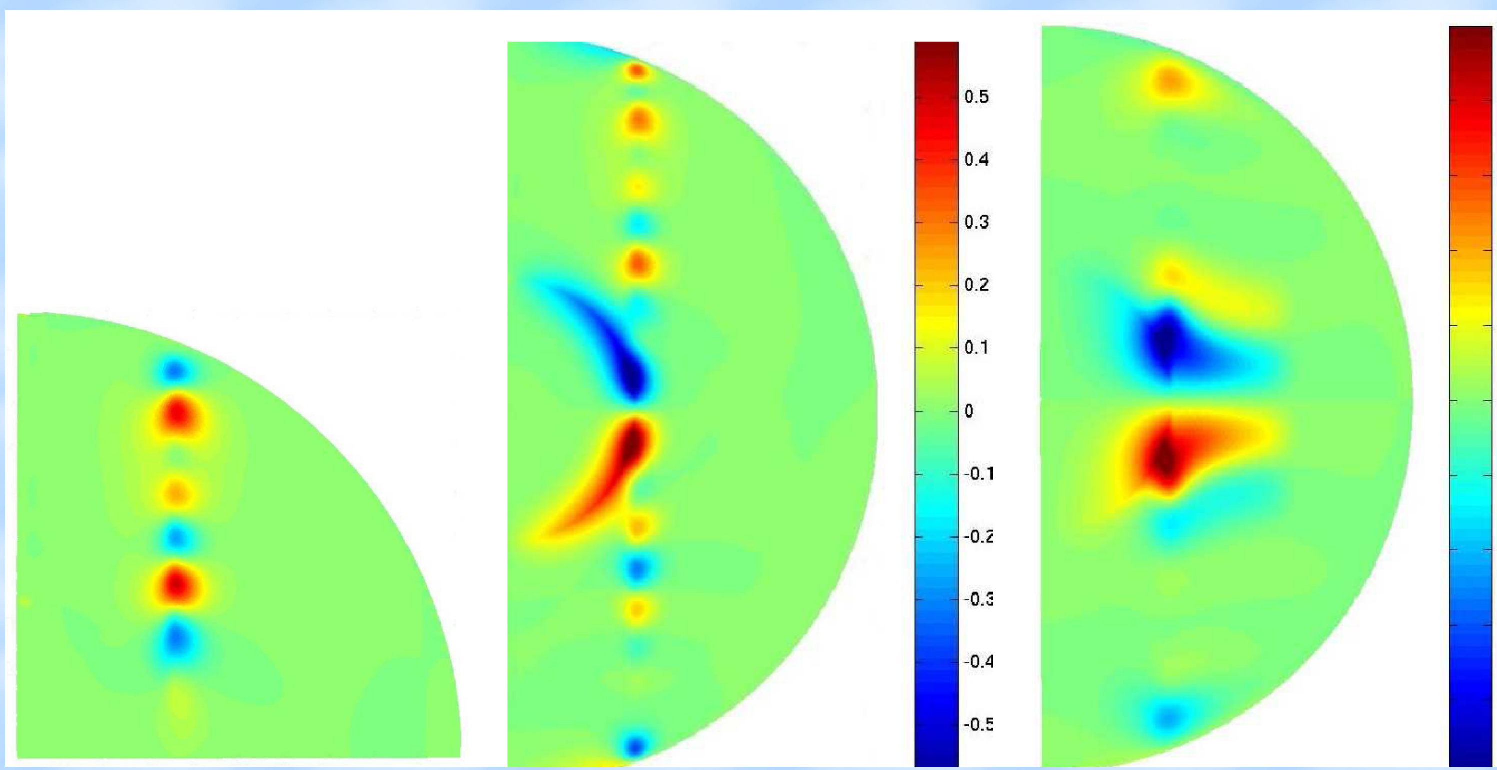

Action of the MS-MRI in the Spherical Couette Flow

Angular velocity

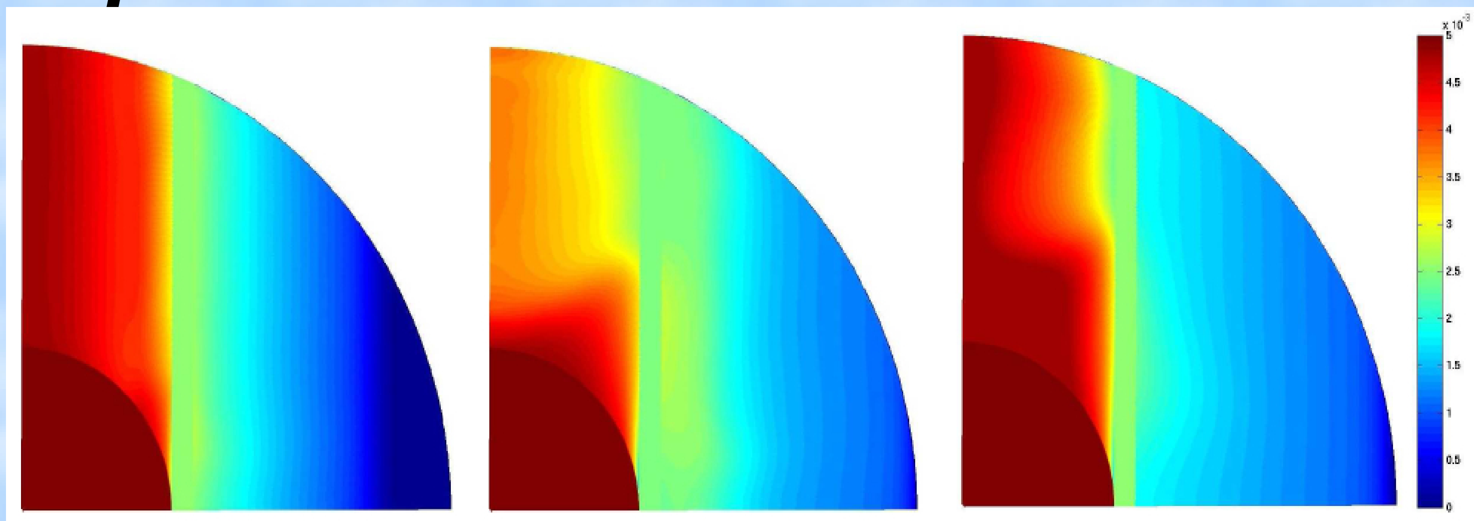

Induced toroidal field

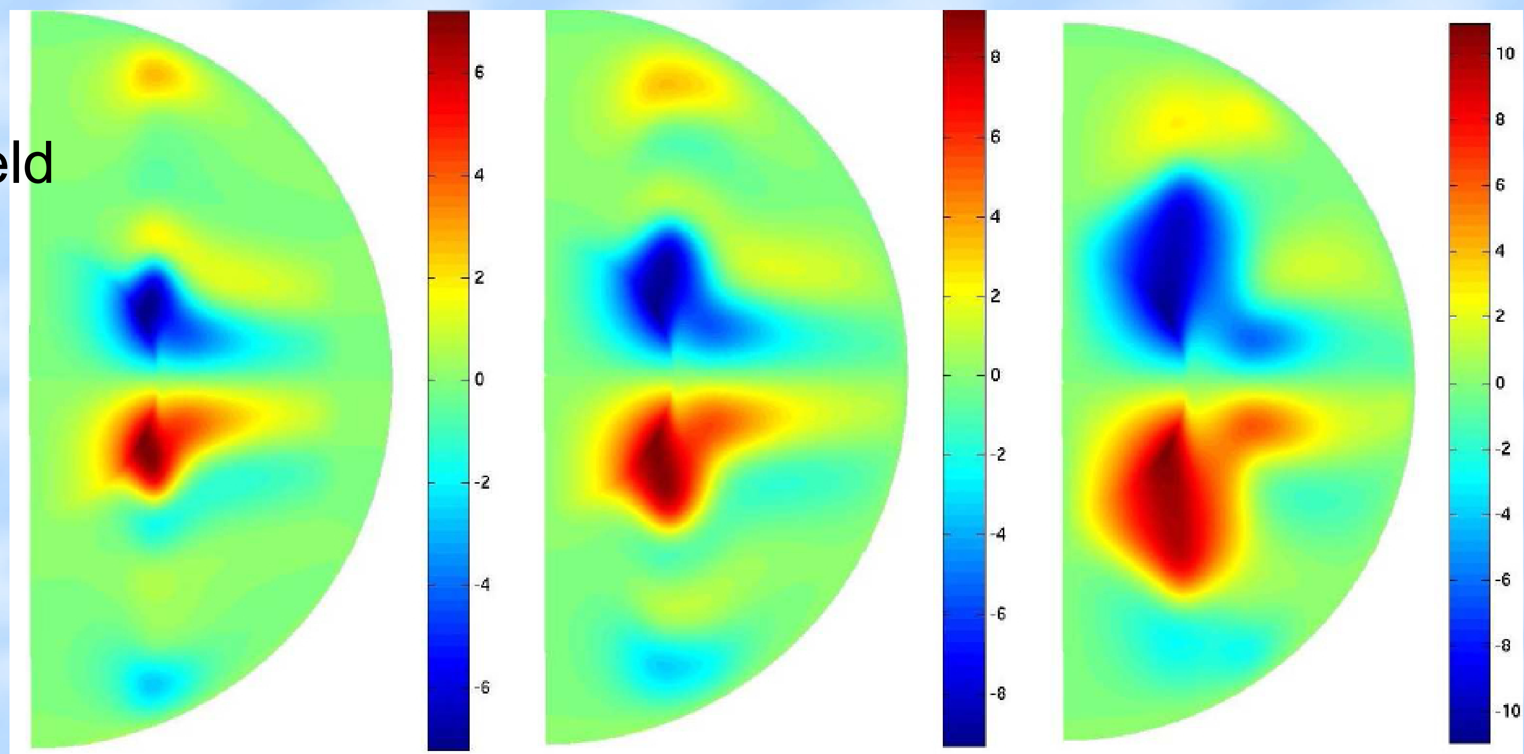

Wave generation

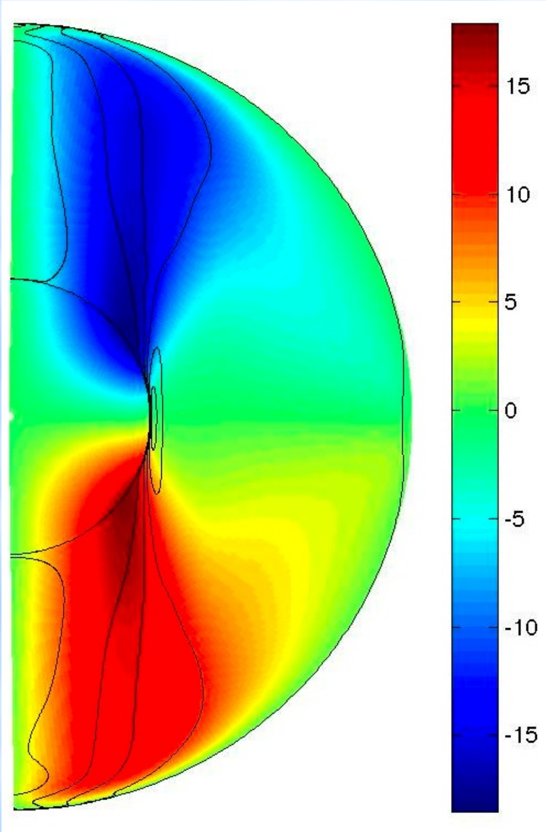

Bφ in color,
Angular velocity contours (black)

Butterfly diagram
bs=br cos(θ)

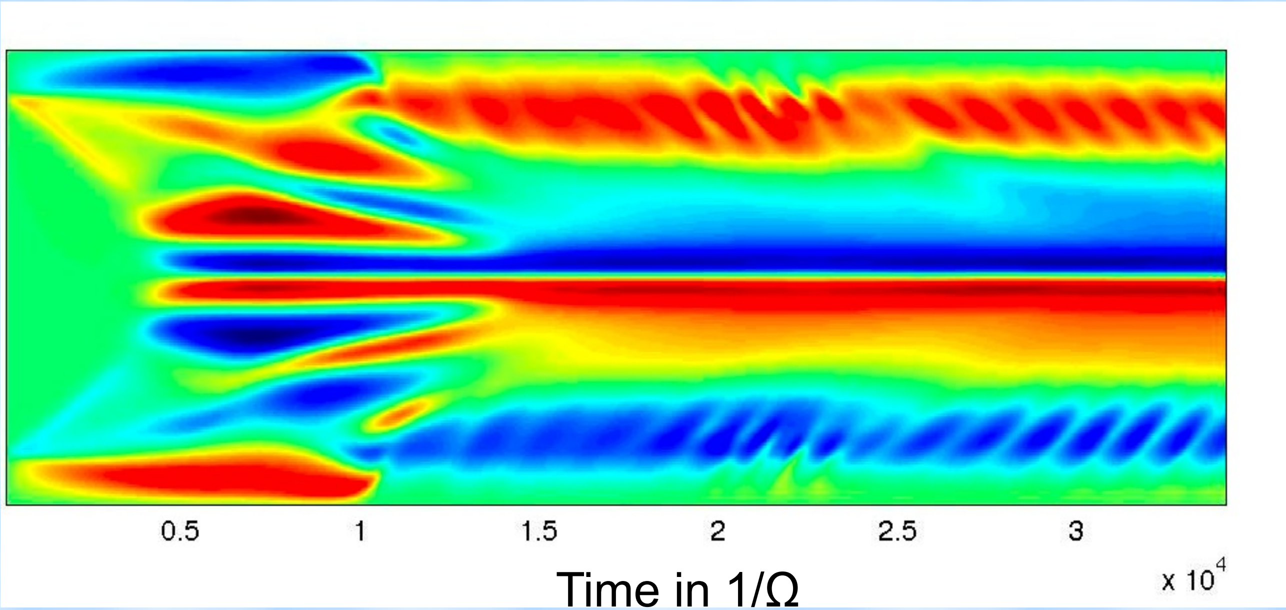

Numerical results for 3D DNS.
Axisymmetric simulations show non-oscillatory field.

Summary (MS-MRI)

- MS-MRI: possible explanation of magnetic variations
- MS-MRI could regulate angular momentum.
- Wave genration, secular variation
- Detection of MS-MRI modes in global numerical dynamos

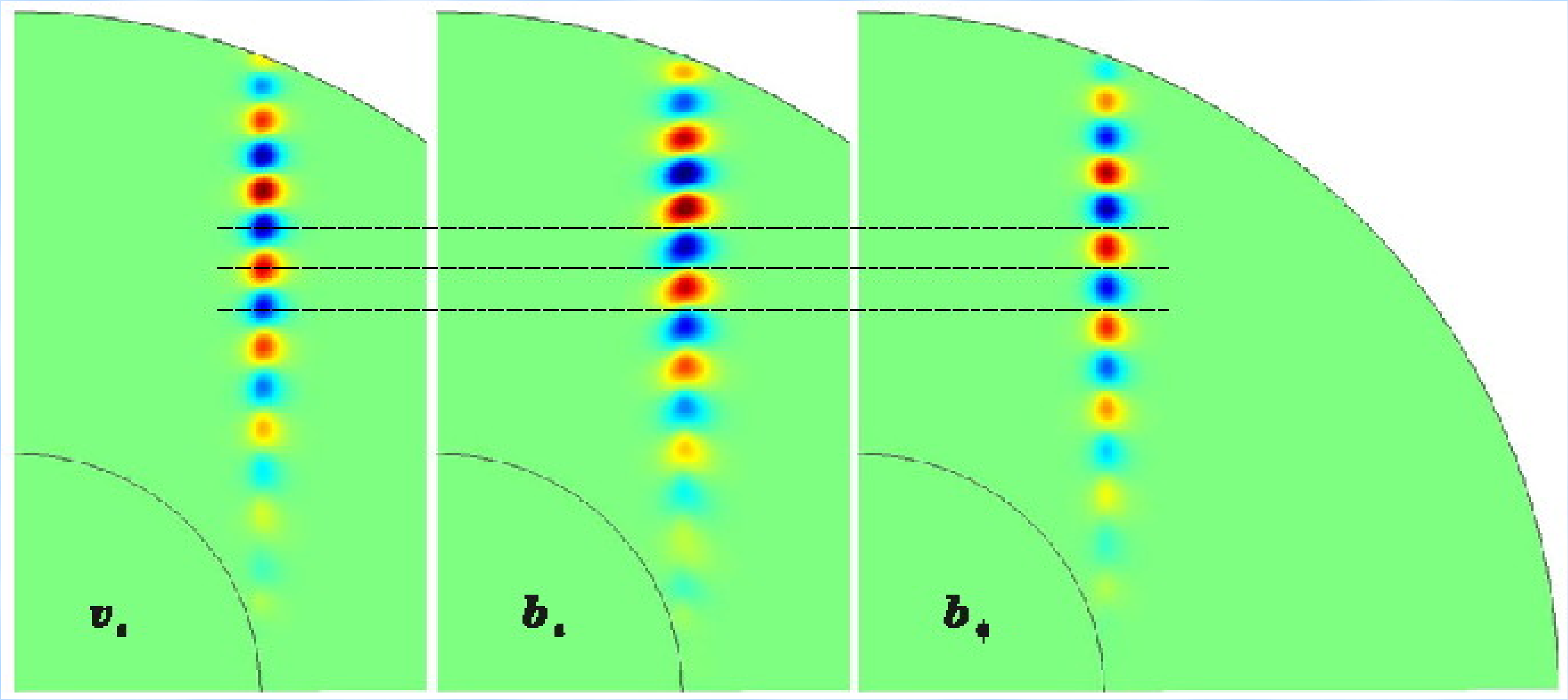

Conclusion

- The observed transition from dipolar to oscillatory dynamos in numerical models is still caused by Rol>0.1.
  - α^2 dynamos could be oscillatory.
- Numerical models with Stress-Free boundary conditions could explain bistability.
- Additional physical effects must be taken into account in order to explain sun-like butterfly diagram.